The influence of the fluid flow velocity and direction on the wave dispersion in the initially inhomogeneously stressed hollow cylinder containing this fluid

Surkay D. Akbarov*[1,2], Jamila N. Imamaliyeva[3a] and Reyhan S. Akbarli[3b]

[1]*Department of Mechanical Engineering, Faculty of Mechanical Engineering, Yildiz Technical University, Yildiz Campus, 34349, Besiktas, Istanbul-Turkey*
[2]*Institute of Mathematics and Mechanics of Science and Education Ministry Republic of Azerbaijan, Baku, Azerbaijan*
[3]*Azerbaijan University of Architecture and Construction, Baku, Azerbaijan*

Abstract. The paper studies the influence of the fluid flow velocity and flow direction in the initial state on the dispersion of the axisymmetric waves propagating in the inhomogeneously pre-stressed hollow cylinder containing this fluid. The corresponding eigenvalue problem is formulated within the scope of the three-dimensional linearized theory of elastic waves in bodies with initial stresses, and with linearized Euler equations for the inviscid compressible fluid. The discrete-analytical solution method is employed, and analytical expressions of the sought values are derived from the solution to the corresponding field equations by employing the discrete-analytical method. The dispersion equation is obtained using these expressions and boundary and related compatibility conditions. Numerical results related to the action of the fluid flow velocity and flow direction on the influence of the inhomogeneous initial stresses on the dispersion curves in the zeroth and first modes are presented and discussed. As a result of the analyses of the numerical results, it is established how the fluid flow velocity and flow direction act on the magnitude of the influence of the initial inhomogeneous stresses on the wave propagation velocity in the cylinder containing the fluid.

Keywords: compressible inviscid fluid; fluid flow velocity; hydro-elastic system; inhomogeneous initial stresses; wave dispersion

1. Introduction

Fundamental theoretical investigations on the dynamics of the "hollow cylinder+fluid" system are required for liquid transportation in various branches of modern industry. These investigations are also required in chemical and nuclear engineering to understand the character of the dynamic interaction between the cylinder and the fluid contained in this cylinder. Importantly in these

∗Corresponding author, Professor, E-mail: akbarov@yildiz.edu.tr
[a]Ph.D., E-mail: ncalila@rambler.ru
[b]Ph.D., E-mail: reyhan.akbarli@azmiu.edu.az

investigations are the studies related to the dispersion of waves propagating in the "hollow cylinder+fluid" systems which originate from the work by Lamb (1898), the results of which create the theoretical base for non-destructive testing of pipelines transporting fluids. Lamb (1898) noted that the first attempt in this field was made by Korteweg in 1878 and he established that the elasticity of the cylindrical shell wall causes to decrease the wave propagation velocity in the compressible inviscid fluid contained in that shell.

The subject of the present paper also relates to the problems of the dispersion of the axisymmetric longitudinal wave propagation in the hollow cylinder with inhomogeneous initial stresses containing an inviscid compressible fluid flowing with constant velocity. It is assumed that the inhomogeneous initial stresses (pre-stresses) in the cylinder are caused by the fluid pressure contained and transported by the cylinder. In order to indicate the place and significance of the present work among other related ones, we briefly review some of them. We begin with the aforementioned paper by Lamb (1898) which studies the dispersion of the axisymmetric waves propagating in the thin cylindrical shell containing an inviscid compressible fluid. Note that in this study, the motion of the shell is described by the Kirchhoff-Love theory and the flexural terms in the equation of motion are neglected.

About 60 years after the appearance of Lamb's work (Lamb 1898), the paper (Lin and Morgan 1956) made a new contribution which consisted of the use of the first-order refined shell theory for describing the motion of the shell in the foregoing hydro-elastic system. At the same time, in the paper by Lin and Morgan (1956), concrete numerical results on the influence of the shear deformation and rotary inertia on the corresponding dispersion curves are presented and discussed.

Later on, researchers in this field focused on the use of more accurate models and equations to describe the fluid flow and the motion of the cylinder. A review of these investigations which were carried out until the last decade of the last century was made in the papers (Sinha *et al.*1992) and (Plona *et al.* 1992). Moreover, in the paper (Sinha *et al.*1992), the dispersion of the axisymmetric longitudinal wave propagating in the hollow cylinder containing the incompressible inviscid fluid was studied theoretically by employing the exact equations and relations of elastodynamics, the experimental testing of which was made in the paper (Plona *et al.* 1992). The more recent research carried out in the papers (Shah 2008, Selvamani 2016, Sandhyarani *et al.* 2019, Kubenko *et al.*2023) and many others therein should also be noted, in which related studies were made for the cases where the cylinder material was a complex one. In the sense of the complexity of the material, the papers (Kocal and Akbarov 2017, 2019) can also be added, in which by utilizing the exact equations and relations of the three-dimensional theory of viscoelasticity, the axisymmetric and flexural waves in the hollow cylinder made of viscoelastic material were investigated.

We also note a series of investigations on the dynamics related to the hydro-elastic systems consisting of the plate and fluid, an example of which are the investigations detailed and made in the papers (Akbarov 2018, Bagno 2017, Bagno 2023, Bagno and Guz 1997, Bagno and Guz 2016, Guz and Bagno 2018, Guz and Bagno 2019) and many others listed therein. There is also a series of investigations such as in the works (Hadzaric *et al.* 2018, Negin and Akbarov 2019) and others listed therein, related to the dynamic problems in the interaction of more complicated flowing mediums and elastic structures.

Now we turn again to the wave dispersion problems in the hydro-elastic systems consisting of the hollow cylinder and fluid. Note that in the cases where the cylinders contain or transport fluids with high pressure and with a certain flow velocity, the cylinders are exposed to pressures from the fluid side. In turn, these pressures cause a stress-strain state in the cylinders which can be taken as the initial stress-strain state with respect to that caused by the additional dynamic perturbations

induced by the acoustic waves propagating in the hydro-elastic systems after these initial stresses appear. When studying the dispersion of the waves propagating in the "cylinder+fluid" systems, one of the main issues is the influence of the initial stresses on this dispersion. Note that the first valuable attempts in this field were made in the papers (Atabek and Lew 1966, Atabek 1968). In the paper (Atabek and Lew 1966), the system is considered which consists of the cylinder made of isotropic and physically linear material and an incompressible Newtonian viscous fluid contained in this cylinder. It is assumed that the cylinder has homogeneous circumferential and longitudinal initial stresses, and how these initial stresses influence the dispersion of the axisymmetric waves propagating in the system is investigated. However, the origins causing the initial stresses are not specified. The motion of the cylinder is described by the thin momentless shell theory, however, the flow of the fluid is described by the linearized Navier-Stokes equations for the incompressible Newtonian fluids. Numerical results on the influence of the initial stresses on the wave propagation velocity and wave amplitude attenuation versus the Womersley number are presented and discussed.

The paper (Atabek 1968) develops the investigation carried out in the paper (Atabek and Lew 1966) for the case where the material of the cylindrical shell is an orthotropic one. The motion of this shell is simulated by a mechanical model consisting of an additional mass, a dashpot, and a spring. The anisotropy of the shell material is taken into consideration only under calculation of the initial stresses. Numerical results that illustrate the influence of the shell material anisotropy on the wave propagation velocity versus the Womersley number are presented and discussed.

The case where the material of the cylinder is highly elastic and incompressible and contains the incompressible viscous Newtonian fluid is considered in the paper (Rvachev 1978). It is assumed that this cylinder has initial homogeneous finite strains in axial and circumferential directions. The equations of motion for the cylinder are described within the scope of the momentless thin shell theory. However, the flow of the fluid is described within the scope of the linearized Navier-Stokes equations. The elasticity relations of the cylinder material are determined through the homogeneous quadratic functions of the normal strains containing three constants of this material. A longwave approximation for obtaining the numerical results that illustrate the wave propagation velocity is also considered, as well as the transmission coefficient versus the square root of the Womersley number.

Note that a model of the highly elastic compressible or incompressible materials for the initially pre-stressed cylinder in contact with the viscous or inviscid compressible fluids is also used in the papers (Bagno and Guz 1982, Bagno *et al.* 1994) and in many others listed therein. It should be noted that in these papers, the motion of the cylinder is described by employing the so-called three-dimensional linearized theory of elastic waves in initially stressed bodies, and numerical results on the dispersion curves are obtained not only for the longwave approximations, but also for all possible wavelength approximations.

Note that all the foregoing investigations related to the wave propagation in the "pre-stressed cylinder+fluid" systems are carried out within the scope of the following two assumptions:

"i") the initial strains (stresses) in the cylinder are homogeneous, and

"ii") in the initial state (i.e., before the wave propagation), the fluid contained in the cylinder is at rest.

It is evident that there are a lot of cases where the cylinders contain flowing fluids with high pressure and this pressure causes inhomogeneous initial stresses within, especially, in the relatively thicker cylinders. At the same time, in the fluid transportation process, this fluid flows with a certain velocity in the cylinder, and this flow takes place before the wave propagation in the

"cylinder+fluid" system starts. Consequently, the question arises as to how the inhomogeneity of the initial stresses in the cylinder are caused by the pressure of the flowing fluid contained in this cylinder and how the velocity of this fluid flow acts on the dispersion of the waves propagating in the "cylinder+fluid" hydro-elastic systems. This question must be studied not only from the point of view of theoretical requirements, but also from the point of view of practical applications.

However, up to now, there are only a few investigations that are related to some particular cases of the formulated question. One of these is made in the paper (Veliyev 2023), in which some numerical results on the influence of the fluid flow speed on the dispersion of the axisymmetric waves propagating in the cylinder containing this fluid are presented. These results are obtained using the exact equations and relations of classic linear elastodynamics, and it was assumed that there are no initial stresses in the cylinder. Consequently, in the paper (Veliyev 2023), the above condition "ii" is violated. Moreover, the paper (Deng and Yang 2013) also violates condition "ii," and the flexural wave propagation dispersion in the buried cylinder containing the flowing fluid is studied. Under this study, it is assumed that the fluid is compressible and inviscid. Fluggle shell theory describes the motion of the cylinder, and the surrounding solid soil is modeled as an elastic matrix using the Winkler model. This paper presents numerical results on the influence of the fluid flow velocity on the wave propagation velocity for the axisymmetric wave propagation case.

According to the authors' best knowledge, until very recently, there were no investigations related to the dispersion of the waves propagating in a fluid-contained cylinder with inhomogeneous initial stresses. The first attempt in this field was made in the paper (Akbarov *et al.* 2021) in which the influence of the inhomogeneous initial stresses in the cylinder caused by the internal hydrostatic pressure on the dispersion of the axisymmetric waves propagating in this cylinder containing the inviscid compressible fluid, is studied. This study is made by utilizing the three-dimensional linearized theory of elastic waves in initially stressed bodies and it is assumed that the fluid in the initial state is at rest. In the paper (Akbarov and Veliyev 2023), a parametric study is made for the problem considered in the paper (Akbarov *et al.* 2021). At the same time, the work by Akbarov *et al.* (2024) investigates the dispersion of quasi-Scholte waves in a hollow cylinder containing a compressible, inviscid fluid parametrically in detail. Moreover, in the paper (Akbarov and Bagirov 2024), dispersion of the axisymmetric waves propagating in the cylinder immersed in the compressible inviscid fluid is studied and it is assumed that as a result of the fluid's hydro-elastic pressure, inhomogeneous initial stresses appear in the cylinder.

However, in the papers (Akbarov *et al.* 2021, Akbarov and Veliyev 2023), it is assumed that the fluid rests in the cylinder. Consequently, in these papers, from the foregoing conditions, only "i" is refused.

Thus, it follows from the above review that there are yet to be investigations that simultaneously take into account the influence of the fluid flow and initial inhomogeneous stresses in the cylinder containing this fluid on the wave dispersion propagating in this cylinder. Thus, in the present paper, attempts are made to study how this flow velocity and flow direction concerning the wave propagation direction act on the influence of the initial inhomogeneous stresses in the cylinder on the dispersion of the axisymmetric waves propagating in this cylinder which contains this flowing fluid. Consequently, the present paper refuses both preceding conditions "i" and "ii".

2. Formulation of the problem

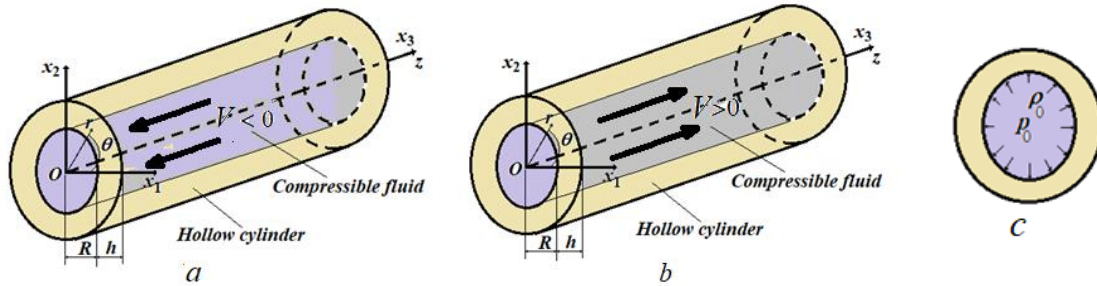Consider the hydro-elastic system consisting of an infinite hollow cylinder and a compressible

Fig. 1 The sketch of the hydro-elastic system under consideration: cylinder containing flowing the fluid flow direction of which is opposite (a) (coincides (b)) with the wave propagation direction; initial pressure and density of the fluid (c)

barotropic inviscid fluid contained in this cylinder. We associate the cylindrical $Or\theta z$ and Cartesian $Ox_1x_2x_3$ ($x_3 = z$) (Fig. 1) systems of coordinates with the central axis of the cylinder. We use the Lagrange and Euler coordinates to describe the motion of the cylinder and fluid, respectively. According to the well-known procedure, we distinguish two states, i.e. the initial and perturbed states in the hydro-elastic system under consideration. Assume that in the initial state, the fluid pressure acts on the interior of the cylinder and this pressure causes a static stress-strain state which is called the "initial stress-strain state". Moreover, assume that in the initial state, the fluid flows in the interior of the cylinder with constant velocity V^0 along the cylinder's axis, according to which, in the initial state the fluid velocity vector is presented as follows

$$V_r^0 = 0, V_\theta^0 = 0, V_z^0 = V^0 = const. \tag{1}$$

As in (1), below we use the upper index "0" for indicating the quantities belonging to the initial state.

Note that the cases where $V^0 < 0$ and $V^0 > 0$ in (1) relate to the fluid flow directions shown in Fig. 1(a) and Fig. 1(b), respectively, i.e., they relate to the cases where the fluid flow direction is opposite to the wave propagation direction (because we will assume that the wave will propagate in the Oz axis (Fig. 1) direction), and the fluid flow direction coincides with the wave propagation direction. The stresses in the cylinder that appear in this initial state as a result of the action of the fluid pressure, according to the monograph (Timoshenko and Goodier 1951), can be presented as follows

$$\sigma_{rr}^0 = \frac{p_0}{(1+h/R)^2-1}\left(1 - \frac{R^2}{r^2}\left(1+\frac{h}{R}\right)^2\right), \quad \sigma_{\theta\theta}^0 = \frac{p_0}{(1+h/R)^2-1}\left(1 + \frac{R^2}{r^2}\left(1+\frac{h}{R}\right)^2\right),$$
$$\sigma_{zz}^0 = \nu(\sigma_{rr}^0 + \sigma_{\theta\theta}^0). \tag{2}$$

In (1) and (2), the conventional notation is used and the geometric parameters R and h which enter into equation (2) are indicated in Fig. 1(a) and (b), but the hydrostatic pressure p_0 in (2) is indicated in Fig. 1(c).

Note that in the paper (Veliyev 2023), it is assumed that $\sigma_{rr}^0 = \sigma_{\theta\theta}^0 = \sigma_{zz}^0 = 0$, i.e., that there are no inhomogeneous initial stresses in the cylinder. However, in the papers (Akbarov *et al.* 2021, Akbarov and Veliyev 2023), it is assumed that the initial inhomogeneous stresses determined in (2) exist in the cylinder. However, the fluid contained in this cylinder rests in the initial state, i.e., in the papers (Akbarov *et al.* 2021, Akbarov and Veliyev 2023), it is assumed that $V_r^0 = V_\theta^0 = V_z^0 = 0$.

The simultaneous satisfaction of the relations (1) and (2) is the main difference between the present investigations from the investigations carried out in the papers (Veliyev 2023) (Akbarov *et al.* 2021, Akbarov and Veliyev 2023). Consequently, the novelty of the present paper's results follows this difference.

Thus, we determine the quantities related to the initial state of the hydro-elastic system under consideration through Eqs. (1) and (2). We assume that after the appearance of this initial state, the hydro-elastic system gets a certain dynamical perturbation, as a result of which the axisymmetric waves propagate therein. It is required to investigate how this initial state influences the dispersion of the waves, that is, to determine how the fluid flowing velocity and flowing direction in the initial state act on the influence of the inhomogeneous initial stresses in the cylinder determined by the relations in (2) on the dispersion of the axisymmetric waves propagating in the cylinder which contains this flowing fluid.

For this investigation, we use the 3D linearized theory of elastic waves in initially stressed bodies for describing the motion of the cylinder and the linearized Euler equations for describing the flow of the inviscid compressible barotropic fluid.

According to works (Eringen and Suhubi 1975, Guz 2004, Akbarov 2015), and others listed therein, we write the 3D linearized equations and corresponding relations describing the motion of the cylinder as follows:

The equations of motion

$$\frac{\partial t_{rr}}{\partial r} + \frac{\partial t_{zr}}{\partial z} + \frac{1}{r}(t_{rr} - t_{\theta\theta}) = \rho \ \frac{\partial^2 u_r}{\partial t^2}, \frac{\partial t_{rz}}{\partial r} + \frac{1}{r}t_{rz} + \frac{\partial t_{zz}}{\partial z} = \rho \ \frac{\partial^2 u_z}{\partial t^2}, \quad (3)$$

where

$$t_{rr} = \sigma_{rr} + \sigma_{rr}^0(r)\frac{\partial u_r}{\partial r}, t_{rz} = \sigma_{rz} + \sigma_{rr}^0(r)\frac{\partial u_z}{\partial r}, t_{\theta\theta} = \sigma_{\theta\theta} + \sigma_{\theta\theta}^0(r)\frac{u_r}{r}, t_{zr} = \sigma_{zr} + \sigma_{zz}^0(r)\frac{\partial u_r}{\partial z},$$
$$t_{zz} = \sigma_{zz} + \sigma_{zz}^0(r)\frac{\partial u_z}{\partial z}, \quad (4)$$

The elasticity relations

$$\sigma_{(jj)} = \lambda \ (\varepsilon_{rr} + \varepsilon_{\theta\theta} + \varepsilon_{zz}) + 2\mu \ \varepsilon_{(jj)}, (jj) = rr; \theta\theta; zz, \ \sigma_{rz} = 2\mu \ \varepsilon_{rz}. \quad (5)$$

The strain-displacement relations

$$\varepsilon_{rr} = \frac{\partial u_r}{\partial r}, \ \varepsilon_{\theta\theta} = \frac{u_r}{r}, \ \varepsilon_{zz} = \frac{\partial u_z}{\partial z}, \ \varepsilon_{rz} = \frac{1}{2}\left(\frac{\partial u_r}{\partial z} + \frac{\partial u_z}{\partial r}\right). \quad (6)$$

In (3) and (4), the notation t_{rr}, t_{rz}, $t_{\theta\theta}$, t_{zr} and t_{zz} shows the components of the non-symmetric Kirchhoff stress tensor and the other notation used in (3)-(6) is conventional. Thus, Eqs. (3)-(6) comprise the complete system of the linearized field equations, in which the wave propagation in the inhomogeneously pre-stressed cylinder is described.

For describing the flow of the fluid, according to the monograph (Guz 2009), we employ the following linearized field (or linearized Euler) equations for barotropic compressible inviscid fluids.

The linearized continuity equation

$$\frac{\partial \rho'}{\partial t} + \rho_0\left(\frac{\partial V_r}{\partial r} + \frac{V_r}{r} + \frac{\partial V_z}{\partial z}\right) + V_z^0\frac{\partial \rho'}{\partial z} = 0. \quad (7)$$

The linearized equations of the fluid flow

$$\frac{\partial V_r}{\partial t} + V_z^0 \frac{\partial V_r}{\partial z} = -\frac{1}{\rho_0}\frac{\partial p'}{\partial r}, \frac{\partial V_z}{\partial t} + V_z^0 \frac{\partial V_z}{\partial z} = -\frac{1}{\rho_0}\frac{\partial p'}{\partial z}. \tag{8}$$

The state equation

$$p' = a_0^2 \rho' \,, a_0^2 = \left(\frac{\partial p'}{\partial \rho'}\right)_0 \tag{9}$$

where a_0 is the sound speed in the fluid.

Note that Eqs. (7)-(9) are written by the Euler coordinates and these equations compose the complete system of equations within the scope of which the flow of the fluid in the perturbed state is described.

Now we add to the foregoing equations the corresponding boundary and compatibility conditions.

The boundary conditions on the external surface of the cylinder are

$$t_{rr}|_{r=R+h} = 0, \ t_{rz}|_{r=R+h} = 0. \tag{10}$$

The compatibility conditions on the interface surface between the fluid and cylinder, i.e., on the internal surface of the cylinder are

$$t_{rr}|_{r=R} = -p', \ t_{rz}|_{r=R} = 0, \ \frac{\partial u_r}{\partial t}\bigg|_{r=R} = V_r|_{r=R}. \tag{11}$$

Assuming that the dynamic perturbations are small, underwriting the compatibility conditions in (11), the differences between the Lagrange and Euler coordinates are neglected. Finally, we write the condition on the boundedness of the quantities related to the fluid at the central axis of the cylinder

$$\{|p'|, |\rho'|, |V_r|, |V_z|\}|_{r=0} < \infty. \tag{12}$$

This completes the mathematical formulation of the problem under consideration.

3. Method of solution to the formulated problem

For the solution to the system of Eqs. (3)-(6), we employ the so-called discrete-analytical method developed and employed in the papers (Akbarov and Bagirov 2019a, 2019b, 2021, 2024, Veliyev and Ipek 2023, Akbarov *et al.* 2021). However, for the solution to the system of Eqs. (7)-(9) related to the fluid flow, we use the presentation presented in the monograph (Guz 2009) for the compressible inviscid fluids.

3.1 Solution to the system of Eqs. (3)-(6).

According to the discrete-analytical solution method, the interval $[R, R + h]$ is divided into an N number of sub-intervals which are determined through the expression $(R + (n-1)h/N) \leq r \leq (R + nh/N)$, where $1 \leq n \leq N$. After this discretization, it is assumed that the inhomogeneous initial stresses determined by expressions (1) and (2) are homogeneous in each sub-interval and the values of these stresses are determined as follows

$$\sigma_{rr}^0(r) \approx \sigma_{rr}^0(r_n), \sigma_{\theta\theta}^0(r) \approx \sigma_{\theta\theta}^0(r_n), \sigma_{zz}^0(r) \approx \sigma_{zz}^0(r_n), r_n = R + (n-1)h/N + h/(2N). \tag{13}$$

Moreover, after the foregoing discretization, full contact conditions are formulated on the

interfaces between the sub-intervals. In other words, we formulate the following conditions instead of conditions (10) and (11)

$$t_{rr}^1|_{r=R} = -p', \ t_{rz}^1|_{r=R} = 0, \ \frac{\partial u_r^1}{\partial t}\Big|_{r=R} = V_r|_{r=R}, \ t_{rr}^1|_{r=R+h/N} = t_{rr}^2|_{r=R+h/N},$$

$$t_{rz}^1|_{r=R+h/N} = t_{rz}^2|_{r=R+h/N}, \ u_r^1|_{r=R+h/N} = u_r^2|_{r=R+h/N},$$

$$u_z^1|_{r=R+h/N} = u_z^2|_{r=R+h/N}, \dots, \quad (14)$$

$$t_{rr}^{n-1}|_{r=R+(n-1)h/N} = t_{rr}^n|_{r=R+(n-1)h/N}, \ t_{rz}^{n-1}|_{r=R+(n-1)h/N} = t_{rz}^n|_{r=R+(n-1)h/N},$$

$$u_r^{n-1}|_{r=R+(n-1)h/N} = u_r^n|_{r=R+(n-1)h/N}, \ u_z^{n-1}|_{r=R+(n-1)h/N} = u_z^n|_{r=R+(n-1)h/N}, \dots,$$

$$t_{rr}^N|_{r=R+h} = 0, \ t_{rz}^N|_{r=R+h} = 0.$$

In (14) there are $4N + 1$ conditions and the number N is determined from the convergence requirement of the numerical results. Note that the upper indices in (14) and below indicate the number of the corresponding sub-interval.

Thus, using the relations in (13), we obtain the following equations of motion from Eqs. (3) and (4) which are satisfied in each nth sub-interval separately

$$\frac{\partial \sigma_{rr}^n}{\partial r} + \sigma_{rr}^0(r_n)\frac{\partial^2 u_r^n}{\partial r^2} + \frac{\partial \sigma_{zr}^n}{\partial z} + \sigma_{zz}^0(r_n)\frac{\partial^2 u_r^n}{\partial z^2} + \frac{1}{r}(\sigma_{rr}^n - \sigma_{\theta\theta}^n) +$$

$$\sigma_{rr}^0(r_n)\frac{1}{r}\frac{\partial u_r^n}{\partial r} - \sigma_{\theta\theta}^0(r_n)\frac{u_r^n}{r^2} = \rho\frac{\partial^2 u_r^n}{\partial t^2}, \quad (15)$$

$$\frac{\partial \sigma_{rz}^n}{\partial r} + \sigma_{rr}^0(r_n)\frac{\partial^2 u_z^n}{\partial r^2} + \frac{1}{r}\sigma_{rz}^n + \sigma_{rr}^0(r_n)\frac{1}{r}\frac{\partial u_z^n}{\partial r} + \frac{\partial \sigma_{zz}^n}{\partial z} + \sigma_{zz}^0(r_n)\frac{\partial^2 u_z^n}{\partial z^2} = \rho\frac{\partial^2 u_z^n}{\partial t^2}.$$

It is necessary to add to these equations the elasticity relation (5), and the relation between the deformations and displacements (6) is rewritten for each subinterval separately. After this addition, for solution to the system of Eqs. (15), (5), and (6), we employ the classical Lame decomposition (see, for instance, the monograph (Eringen and Suhubi 1975), which for the axisymmetric problems can be written as follows

$$u_r^n = \frac{\partial \Phi^n}{\partial r} + \frac{\partial^2 \Psi^n}{\partial r \partial z}, \ u_z^n = \frac{\partial \Phi^n}{\partial z} - \frac{\partial^2 \Psi^n}{\partial r^2} - \frac{\partial \Psi^n}{r \partial r}. \quad (16)$$

Using the Eqs. (6) and (5), we obtain the following equations for the potentials Φ^n and Ψ^n from the equations in (15)

$$\left(1 + \frac{\sigma_{rr}^0(r_n)}{\lambda+2\mu}\right)\frac{\partial^2 \Phi^n}{\partial r^2} + \left(1 + \frac{\sigma_{\theta\theta}^0(r_n)}{\lambda+2\mu}\right)\frac{\partial \Phi^n}{r\partial r} + \left(1 + \frac{\sigma_{zz}^0(r_n)}{\lambda+2\mu}\right)\frac{\partial^2 \Phi^n}{\partial z^2} = \frac{1}{(c_1)^2}\frac{\partial^2 \Phi^n}{\partial t^2},$$

$$\left(1 + \frac{\sigma_{rr}^0(r_n)}{\mu}\right)\frac{\partial^2 \Psi^n}{\partial r^2} + \left(1 + \frac{\sigma_{\theta\theta}^0(r_n)}{\mu}\right)\frac{\partial \Psi^n}{r\partial r} + \left(1 + \frac{\sigma_{zz}^0(r_n)}{\mu}\right)\frac{\partial^2 \Psi^n}{\partial z^2} = \frac{1}{(c_2)^2}\frac{\partial^2 \Psi^n}{\partial t^2}, \quad (17)$$

where $c_1 = \sqrt{\frac{(\lambda+2\mu)}{\rho}}$ and $c_2 = \sqrt{\frac{\mu}{\rho}}$.

It follows from the equations in (17) that in the cases where the initial stresses are absent, i.e., in the cases where $\sigma_{zz}^0(r_n) = 0, \sigma_{rr}^0(r_n) = 0$, and $\sigma_{\theta\theta}^0(r_n) = 0$, the equations in (17) coincide with the corresponding equations of classical elastodynamics (see, for instance the monograph (Eringen and Suhubi 1975)).

Representing the functions $\Phi^n, u_r^n, \sigma_{rr}^n, \sigma_{\theta\theta}^n$ and σ_{zz}^n with the multiplying $\sin(kx - \omega t)$ and the functions Ψ^n, u_z^n and σ_{rz}^n with the multiplying $\cos(kx - \omega t)$, and denoting the amplitudes of the corresponding quantities with the same symbols, we obtain the following equations for the

amplitudes of the potentials Φ^n and Ψ^n

$$\frac{d^2\Phi^n}{d(r_2)^2} + \frac{\alpha_1(r_n)}{r_2}\frac{d\Phi^n}{dr_2} + \Phi^n = 0, \quad \frac{d^2\Psi^n}{d(r_1)^2} + \frac{\alpha(r_n)}{r_1}\frac{d\Psi^n}{dr_1} + \Psi^n = 0, \quad (18)$$

where

$$\alpha(r_n) = \frac{1+\sigma_{\theta\theta}^0(r_n)/\mu}{1+\sigma_{rr}^0(r_n)/\mu}, \beta(r_n) = \frac{1+\sigma_{zz}^0(r_n)/\mu}{1+\sigma_{rr}^0(r_n)/\mu}, r_1^n = kr\sqrt{\frac{c^2}{(c_2)^2(1+\sigma_{rr}^0(r_n)/\mu)} - (\beta(r_n))^2},$$

$$c = \omega/\kappa, \alpha_1(r_n) = \frac{1+\sigma_{\theta\theta}^0(r_n)/(\lambda+2\mu)}{1+\sigma_{rr}^0(r_n)/(\lambda+2\mu)}, \beta_1(r_n) = \frac{1+\sigma_{zz}^0(r_n)/(\lambda+2\mu)}{1+\sigma_{rr}^0(r_n)/(\lambda+2\mu)} \quad (19)$$

$$r_2^n = kr\sqrt{\frac{c^2}{(c_1)^2(1+\sigma_{rr}^0(r_n)/(\lambda+2\mu))} - (\beta_1(r_n))^2}.$$

Thus, according to (Akbarov and Bagirov 2019b, Watson 1966), the solution to the equations in (19) are found as follows.

$$\Phi^n = A_1^n(r_2)^{\gamma_1(r_n)}E_{\gamma_1(r_n)}(r_2^{n_i}) + A_2^n(r_2)^{\gamma_1(r_n)}F_{\gamma_1(r_n)}(r_2^n) \quad (20)$$

$$\Psi^n = B_1^n(r_1)^{\gamma\ (r_n)}E_{\gamma\ (r_n)}(r_1^n) + B_2^n(r_1)^{\gamma\ (r_n)}F_{\gamma\ (r_n)}(r_1^n) \quad (21)$$

where A_1^n, A_2^n, B_1^n and B_2^n are unknown constants and

$$\gamma_1(r_n) = (1 - \alpha_1(r_n))/2, \gamma(r_n) = (1 - \alpha(r_n))/2,$$

$$E_{\gamma_1(r_n)}(r_2^n) = \begin{cases} J_{\gamma_1(r_n)}(r_2^n) if (r_2^n)^2/r^2 > 0 \\ I_{\gamma_1(r_n)}(r_2^n) if (r_2^n)^2/r^2 < 0 \end{cases}'$$

$$F_{\gamma_1(r_n)}(r_2^n) = \begin{cases} Y_{\gamma_1(r_n)}(r_2^n) if (r_2^n)^2/r^2 > 0 \\ K_{\gamma_1(r_n)}(r_2^n) if (r_2^n)^2/r^2 < 0 \end{cases}' \quad (22)$$

$$E_{\gamma(r_n)}(r_1^n) = \begin{cases} J_{\gamma(r_n)}(r_1^n) if (r_1^n)^2/r^2 > 0 \\ I_{\gamma(r_n)}(r_1^n) if (r_1^n)^2/r^2 < 0 \end{cases}'$$

$$F_{\gamma(r_n)}(r_1^{n_i}) = \begin{cases} Y_{\gamma(r_{n_i})}(r_1^n) if (r_1^n)^2/r^2 > 0 \\ K_{\gamma(r_n)}(r_1^n) if (r_1^{n_i})^2/r^2 < 0 \end{cases}$$

In (22), $J_\delta(x)$ and $I_\delta(x)$ are the Bessel and modified Bessel functions of the first kind, however, $Y_\delta(x)$ and $K_\delta(x)$ are the Bessel and modified Bessel functions of the second kind.

Substituting these solutions into the presentations in (16), we determine the expressions for the displacements, and then using the relations in (6) and (5), we obtain the expressions for the stresses within each sub-interval. The explicit forms of these expressions for the displacements and stresses which enter the contact and compatibility conditions (14) are given in Appendix A through the formulae (A1) and (A2), respectively.

In this way we determine the analytic expressions for the displacements and stresses in each sub-interval into which the region $[R, R + h]$ is divided.

3.2 Solution to the field equations related to the fluid flow

For solution to equations in (7), according to (Guz 2009), we use following representations.

$$\rho' = a_0^{-2}\rho_0\left(-V_z^0\frac{\partial}{\partial z} - \frac{\partial}{\partial t}\right)\Phi_f, \; p' = \rho_0\left(-V_z^0\frac{\partial}{\partial z} - \frac{\partial}{\partial t}\right)\Phi_f, \; V_r = \frac{\partial}{\partial r}\Phi_f, \; V_z = \frac{\partial}{\partial z}\Phi_f \qquad (23)$$

where

$$\left[\Delta - \frac{1}{a_0^2}\left(\frac{\partial}{\partial t} + V_z^0\frac{\partial}{\partial z}\right)^2\right]\Phi_f = 0 \;, \Delta = \frac{\partial^2}{\partial r^2} + \frac{1}{r}\frac{\partial}{\partial r} + \frac{\partial^2}{\partial z^2}. \qquad (24)$$

Representing the functions V_z, p' and ρ' by the multiplying $\sin(kz - \omega t)$, and the functions Φ_f and V_r by the multiplying $\cos(kz - \omega t)$, we obtain the following equation from (24) for Φ_{f1} (where $\Phi = \Phi_{f1}(r)\cos(kz - \omega t)$)

$$\left(\frac{d^2}{dr_3^2} + \frac{1}{r_3}\frac{d}{dr_3} + 1\right)\Phi_{f1}(r) = 0 \;, r_3 = kr\sqrt{\left(\frac{c}{a_0}\right)^2 - 2\frac{c}{a_0}\frac{V_z^0}{a_0} + \left(\frac{V_z^0}{a_0}\right)^2 - 1}. \qquad (25)$$

According to the conditions in (12), the solution to Eq. (25) is found as follows

$$\Phi_{f1}(r) = \begin{cases} FJ_0(r_3) \; if \; r_3^2 > 0 \\ FI_0(r_3) \; if \; r_3^2 < 0 \end{cases} \qquad (26)$$

where $J_0(r_3)$ ($I_0(r_3)$) is the Bessel (modified Bessel) function of the first kind with the zeroth order and F is an unknown constant.

Using the expression (26) and substituting $\Phi = \Phi_{f1}(r)\cos(kz - \omega t)$ into the equations in (23), we obtain the following expressions for the sought values related to the fluid

$$p' = \rho_0(V_z^0 k + \omega)\sin(kz - \omega t)\begin{cases} FJ_0(r_3) \; if \; r_3^2 > 0 \\ FI_0(r_3) \; if \; r_3^2 < 0 \end{cases},$$

$$\rho' = a_0^{-2}\rho_0(V_z^0 k + \omega)\sin(kz - \omega t)\begin{cases} FJ_0(r_3) \; if \; r_3^2 > 0 \\ FI_0(r_3) \; if \; r_3^2 < 0 \end{cases}, \qquad (27)$$

$$V_r = k\frac{dr_3}{dr}\cos(kz - \omega t)\begin{cases} -FJ_1(r_3) \; if \; r_3^2 > 0 \\ FI_1(r_3) \; if \; r_3^2 < 0 \end{cases}, \; V_z = -k\sin(kz - \omega t)\begin{cases} FJ_0(r_3) \; if \; r_3^2 > 0 \\ FI_0(r_3) \; if \; r_3^2 < 0 \end{cases}$$

Note that in (27), ρ_0 shows the density of the fluid in the initial state.

This completes the determination of the quantities related to the fluid flow in the perturbed state.

3.3 Obtaining the dispersion equation

As follows from the foregoing discussions and solution procedures, the analytical expressions of the sought values contain $4N + 1$ number of unknown constants and these constants are A_1^n, A_2^n, B_1^n, B_2^n ($n = 1,2,\dots,N$) and F. Substituting the expressions in (A1) and (A2), and in (27) into the conditions indicated in (14), we obtain the system of homogeneous algebraic equations with respect to these unknown constants. According to the well-known procedure, equating to zero the determinant of the coefficient matrix of this system, we obtain the dispersion equation. This equation can be formally presented as follows

$$det(a_{nm}(c/c_2, kR, V^0/a_0, p_0/\mu, \frac{\rho}{\rho_0, h/R}, a_0/c_2)) = 0, n; m = 1,2,\dots,4N + 1 \qquad (28)$$

The explicit expressions of the components a_{nm} can be easily determined from the formulae (A1) and (A2) in Appendix A and in (27). Therefore, these expressions are not given here.

The dispersion equation (28) is solved numerically by employing the "bi-section" method.

4. Numerical results and discussions

4.1 Selection of the materials and validation of the calculation algorithm

We assume that the material of the cylinder is steel with the Lame constants $\lambda = 1.075 \times 10^{11}$ Pa and $\mu = 0.77 \times 10^{11}$ Pa, the material density is $\rho = 7910 \frac{\text{kg}}{\text{m}^3}$, and the fluid is water with sound speed $a_0 = 1495 \frac{\text{m}}{\text{sec}}$ and density $\rho_0 = 1000 \frac{\text{kg}}{\text{m}^3}$. All numerical results, which will be discussed in the present paper, are obtained for these materials. Note that these pairs of materials are also selected in the papers (Akbarov *et al.* 2021, Sinha *et al.* 1992) for obtaining concrete numerical results, which we will also use for validation of the algorithm and PC programs used in the present investigation. In obtaining the numerical results, the magnitude of the fluid velocity is estimated through the ratio V^0/a_0 and the magnitude of the initial inhomogeneous stresses in the cylinder is estimated through the ratio p_0/μ. Below, the case where $V^0/a_0 < 0$ ($V^0/a_0 > 0$) relates to the case where the fluid flow velocity direction is opposite (coincides) with the wave propagation direction.

Unfortunately, except for a few numerical results presented in the paper (Veliyev 2023) and the investigations carried out in the paper (Deng and Yang 2013), we have not found any concrete investigations related to the influence of the fluid flow velocity on the wave propagation velocity in the cylinder containing this fluid. Note that the numerical results which will be presented and discussed below in particular cases, i.e., where $\{ p_0/\mu = 0 \,; V^0/a_0 \neq 0 \}$ coincide with the corresponding results obtained in the paper (Veliyev 2023). Therefore, here we do not consider testing the PC programs and calculation algorithm used with the results obtained in the paper (Veliyev 2023). Moreover, the results presented in the paper (Deng and Yang 2013) are obtained within the framework of the approximate shell theory in the case where $\{p_0/\mu = 0; V^0/a_0 > 0\}$.

Therefore, comparison of the present results with the results obtained in the paper (Deng and Yang 2013) can be made only in the qualitative sense, which also will be made below under discussion of the numerical results related to the case where $V^0/a_0 > 0$. Based on these statements, for illustration of the aforementioned validation, we use the results obtained in the paper (Sinha *et al.* 1992) which corresponds to the case where $p_0/\mu = 0$ and $V^0/a_0 = 0$.

Thus, for validation of the PC programs and solution method used in the present investigation, we consider the dispersion diagrams illustrated in Fig. 2 which are obtained in the case where $h/R = 0.2$ and $p_0/\mu = 0$ for the zeroth, first, and second modes under $V^0/a_0 = 0.0$; - 0.05; - 0.10 and - 0.15. Note that the results regarding the case where $V^0/a_0 = 0.0$ are also obtained in the paper (Sinha *et al.* 1992) and coincide completely with the present ones. At the same time, the results shown in Fig. 2 are obtained with the same PC programs which are used in the case where $V^0/a_0 = 0.0$ and $p_0/\mu > 0$, which are discussed in the paper (Akbarov *et al.* 2021). We note that all the numerical results in the present paper, as in the paper (Akbarov *et al.* 2021), are obtained in the case where $N = 54$, i.e., in the case where the number of sub-intervals into which the region $[R, R + h]$ is divided is equal to 54.
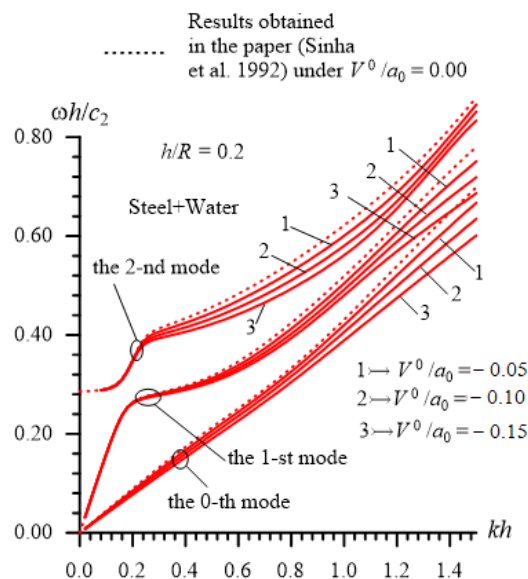
Fig. 2 Dispersion diagrams obtained for the zeroth, first, and second modes for various values of the ratio V^0/a_0 in the case where $p_0/\mu = 0$

Thus, it follows from the results illustrated in Fig. 2 that an increase in the absolute values of V^0/a_0 causes the values of the wave propagation velocity to decrease. We attempt to explain this character of the influence of the fluid flow on the wave propagation velocity and consider the dispersion curves illustrated in Fig. 3. These relate to the axisymmetric longitudinal waves propagating in the Oz axis direction in the fluid, which is in the absolutely rigid hollow cylinder with internal radius R in the cases where the fluid in the initial state flows with constant velocity V^0 in the direction which is opposite the wave propagation direction (Fig. 3(a)), and in the direction which coincides with the wave propagation direction (Fig. 3b). Note that under obtaining these results, the condition $V_r = 0$ is assumed at $r = R$. Thus, it follows from Fig. 3 that if, in the initial state, the fluid flow direction is opposite (Fig. 3(a)) (coincides with (Fig. 3(b))) the wave propagation direction, then the fluid flow in the initial state leads to a decrease (an increase) in the wave propagation velocity in the fluid which is in the absolute rigid cylinder. Moreover, the magnitudes of this "decrease" and "increase" grow monotonically with the fluid flow velocity V^0 in the initial state. This property of the fluid flow in the initial state also decreases or increases in the wave propagation velocity in the elastic cylinder containing this fluid. Therefore, the results illustrated in Fig. 2 can be explained, with the "increase" or "decrease" of the wave propagation velocity in the fluid. However, in the case where the fluid is in the elastic cylinder, the influence of the fluid flow velocity on the wave propagation velocity is more complicated than in the case where the flowing fluid is in the rigid hollow cylinder.

The results illustrated in Fig. 3 can be explained by "slowing down" ("increasing") the motion speed of the wave front in the excited state, i.e., under the wave propagation process in the wave propagation direction, i.e., in the Oz axis direction, because the direction of the fluid flow in the initial state is opposite (coincides with) the direction of the wave propagation. This explanation of the numerical results illustrated in Fig. 3 agrees with well-known physico-mechanical considerations.
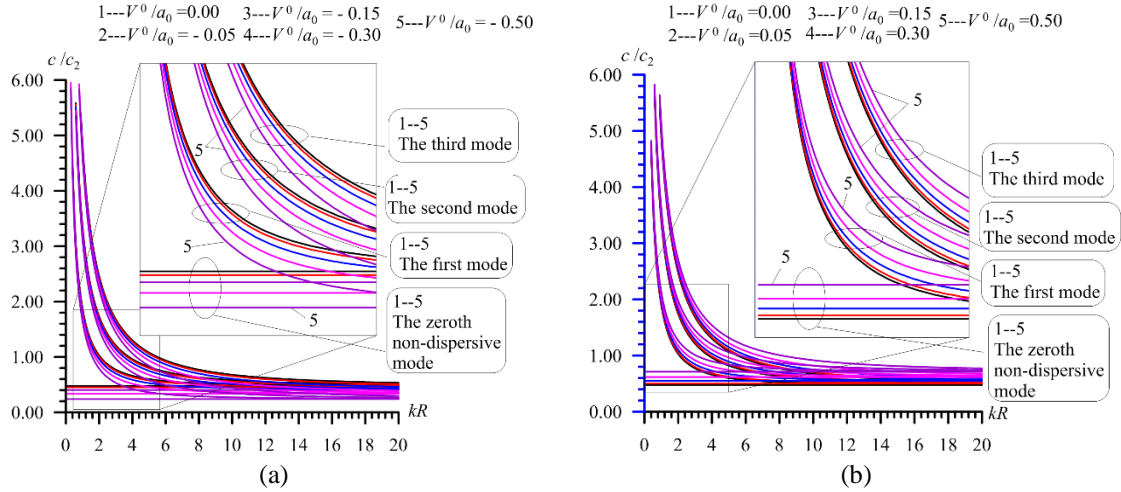
Fig. 3 Dispersion curves of the waves propagating in the fluid which is in the absolutely rigid hollow cylinder with an internal radius R

Note that numerical examples illustrating the increased wave propagation velocity in the fluid which is in an elastic hollow cylinder in the case where $V^0/a_0 > 0$, with increases in the values of V^0/a_0, will be illustrated below.

In this way, we validate the reliability of the algorithm and PC programs used in the present investigations.

4.2 Numerical results obtained in the case where $V^0/a_0 < 0$

First, we consider the dispersion curves, i.e., the graphs of the dependence between the ratio c/c_2 and dimensionless wavenumber kR (where k is the wavenumber) obtained for the so-called zeroth mode. Recall that this mode is also called the quasi-Scholte waves mode and appears as a result of the fluid–solid dynamic interaction. The graphs are given in Fig. 4, and the results grouped by the letters *a*, *b*, and *c*, relate to the cases where $h/R = 0.1$, 0.2 and 0.3, respectively. The results for each selected value of the ratio h/R in Fig. 4 are obtained for various values of the fluid flowing velocity in the initial state, i.e., for various minus values of V^0/a_0 and for various values of the ratio p_0/μ which characterizes the magnitude of the initial inhomogeneous stresses in the cylinder.

Analysis of the numerical results illustrated in Fig. 4 allows us to write the following relations, where for each selected value of the ratio p_0/μ, take place

$$c/c_2|_{V^0/a_0=0.00} > c/c_2|_{V^0/a_0=-0.05} > c/c_2|_{V^0/a_0=-0.10} > c/c_2|_{V^0/a_0=-0.15} \tag{29}$$

There exists such a value of kR (denote it by $(kR)*$) after which, i.e., in the cases where $kR > (kR)*$ for each fixed value of the ratio V^0/a_0, the following relations take place

$$c/c_2|_{10^6 p_0/\mu=0.0} < c/c_2|_{10^6 p_0/\mu=1.0} < c/c_2|_{10^6 p_0/\mu=5.0} < c/c_2|_{10^6 p_0/\mu=10.0} < c/$$
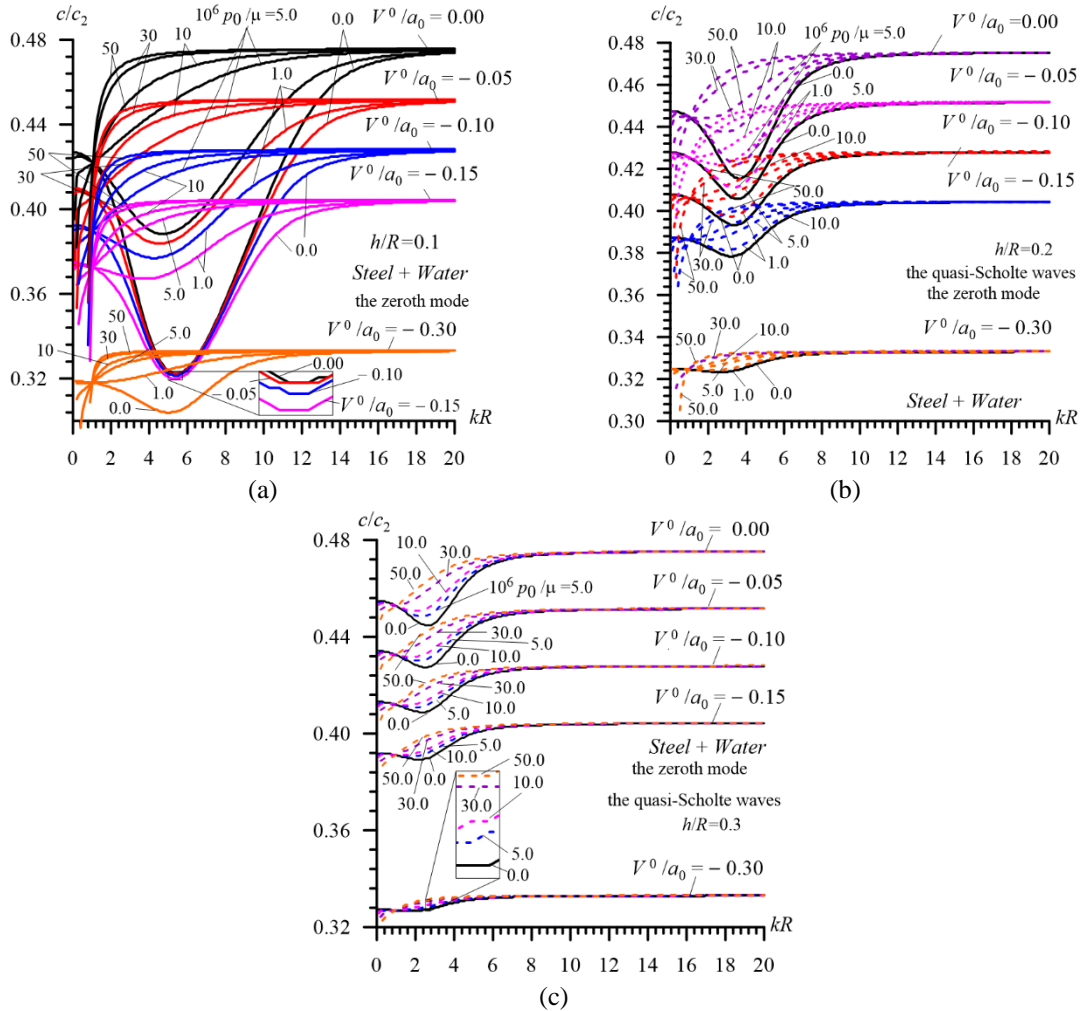$$c_2|_{10^6 p_0/\mu=30.0} < c/c_2|_{10^6 p_0/\mu=50.0} \tag{30}$$

Fig. 4 Dispersion curves in the zeroth mode under $h/R = 0.1$(a), 0.2(b) and 0.3(c)

However, in the cases where $kR < (kR)*$, the relations (30) become the opposite, i.e.

$$c/c_2|_{10^6 p_0/\mu=0.0} > c/c_2|_{10^6 p_0/\mu=1.0} > c/c_2|_{10^6 p_0/\mu=5.0} > c/c_2|_{10^6 p_0/\mu=10.0} > c/$$
$$c_2|_{10^6 p_0/\mu=30.0} > c/c_2|_{10^6 p_0/\mu=50.0}$$

(31)

Note that in the case where $kR = (kR)*$, the initial stresses in the cylinder do not influence the propagation velocity of the quasi-Scholte waves.

If we compare the graphs shown in Fig. 4 (a), (b), and (c), we can see that the size of the difference between the minimum velocity of the quasi-Scholte waves and the velocity of the corresponding Scholte waves decreases with h/R. Additionally, this comparison shows that the graphs of the dispersion curves obtained for the concrete selected value of V^0/a_0 are clearly separate from the graphs obtained for the other values of V^0/a_0, i.e., the graphs related to each selected V^0/a_0 shift completely "down" with h/R.
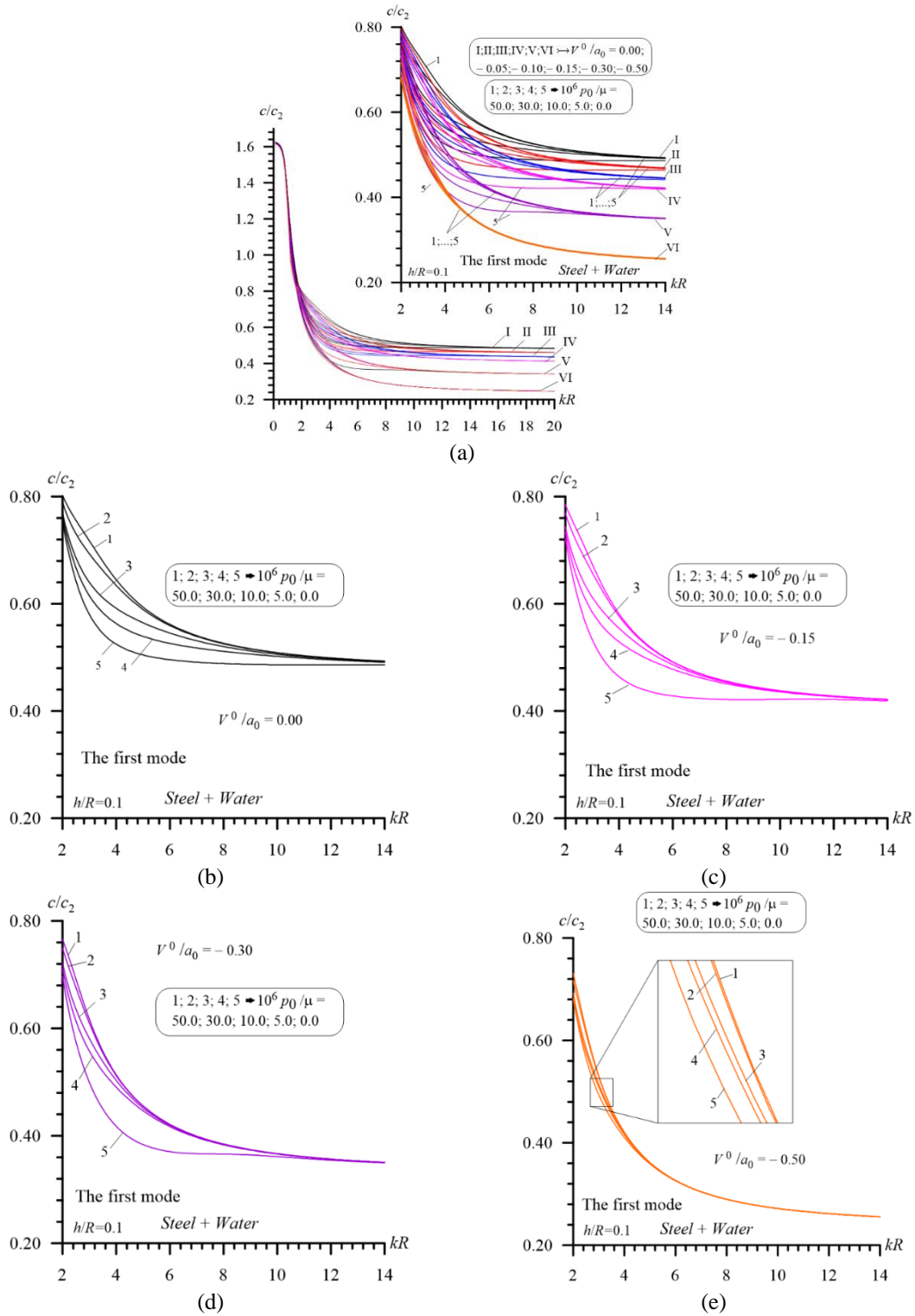
Fig. 5 Dispersion curves for the first mode obtained under $h/R = 0.1$

At the same time, the graphs given in Fig. 4 show that the velocity of the Scholte waves propagating near the interface plane between the flowing fluid and elastic half-spaces decreases with the absolute values of the fluid flowing velocity V^0/a_0.

It also follows from the graphs given in Fig. 4 that the length of the region $0 < kR < (kR)_1$ into which the influence of the initial stresses, i.e., p_0/μ on the dispersion curves on the velocity of the wave propagation is significant, decreases with the ratio h/R.

Furthermore, it follows from the analyses of the results given in Fig. 4, that an increase in the absolute values of V^0/a_0 causes a monotonic decrease in the magnitude of the influence of the ratio p_0/μ on the wave propagation velocity. This is the main qualitative effect of the action of the fluid flow velocity in the case where $V^0/a_0 < 0$ on the influence of the ratio p_0/μ on the wave propagation velocity in the zeroth mode.

Moreover, the numerical results obtained for all the selected values of the ratio h/R under $V^0/a_0 = -0.5$ show that the dispersion curve related to the zeroth mode becomes non-dispersive. The wave propagation velocity on this curve is equal to the corresponding velocity of the non-dispersive wave propagating in the fluid in the rigid cylinder (Fig. 3(a)). Consequently, under relatively great values of the fluid flow velocity in the direction that is opposite to the direction of the wave propagation direction, the fluid flow leads to the dispersive character of the zeroth mode disappearing. Note that this is observed in all the values of the ratio p_0/μ, and the propagation velocity of the non-dispersive wave does not depend on this ratio. In connection with this, in Fig. 4, the dispersion curves related to the case where $V^0/a_0 = -0.5$ are not shown.

This completes the analyses of the results related to the zeroth mode.

Now we consider the dispersion curves related to the first mode. The graphs of the this mode are given in Figs. 5, 6 and 7 in the cases where $h/R = 0.10, 0.20$, and 0.30, respectively. These graphs are constructed for various values of p_0/μ under $V^0/a_0 = 0.0$; -0.05; -0.10, -0.15, -0.30 and -0.50. Note that in the figures indicated by the letter "*a*", the general presentation of the corresponding dispersion curves constructed for various minus values of the fluid flow velocity V^0/a_0 and the various values of the ratio p_0/μ in the case where $0 < kR \le 20$ as well as the parts of these dispersion curves on which the influence of the initial inhomogeneous stresses is considerable, are shown. However, in the figures indicated by letters "*b*", "*c*", "*d*", and "*e*", these parts of the dispersion curves are shown in the cases where $V^0/a_0 = 0.0$, -0.15, -0.30, and -0.50, respectively. These illustrations show more precisely the influence of the ratio p_0/μ on the parts of the dispersion curves. Consequently, comparison of the results given in the figures indicated by the letters "*b*", "*c*", "*d*", and "*e*" may allow us to make some conclusions on the magnitude of the influence of the initial inhomogeneous stresses in the cylinder depending on the initial fluid velocity.

According to Figs. 5, 6, and 7, in the first mode, the aforementioned parts in which the magnitude of the influence of the ratio p_0/μ on the dispersion curves is considerable, relate to the cases where $2.0 < kR \le (kR)'$. In these relations, the values of $(kR)'$ depend on the ratio h/R, i.e., the value of $(kR)'$ decreases with h/R. With respect to the cases under consideration, in the first mode, it can be concluded that $(kR)' = 14, 10$ and 6 for the cases where $h/R = 0.1, 0.2$ and 0.3, respectively.

Comparison of the graphs obtained for the first mode and grouped by the letters "*b*", "*c*", "*d*", and "*e*" with each other shows that in the first mode, an increase in the absolute values of the fluid flow velocity leads to a decrease in the magnitude of the influence of the inhomogeneous initial stresses in the cylinder on the wave propagation velocity. The values of $(kR)'$ depend on the ratio
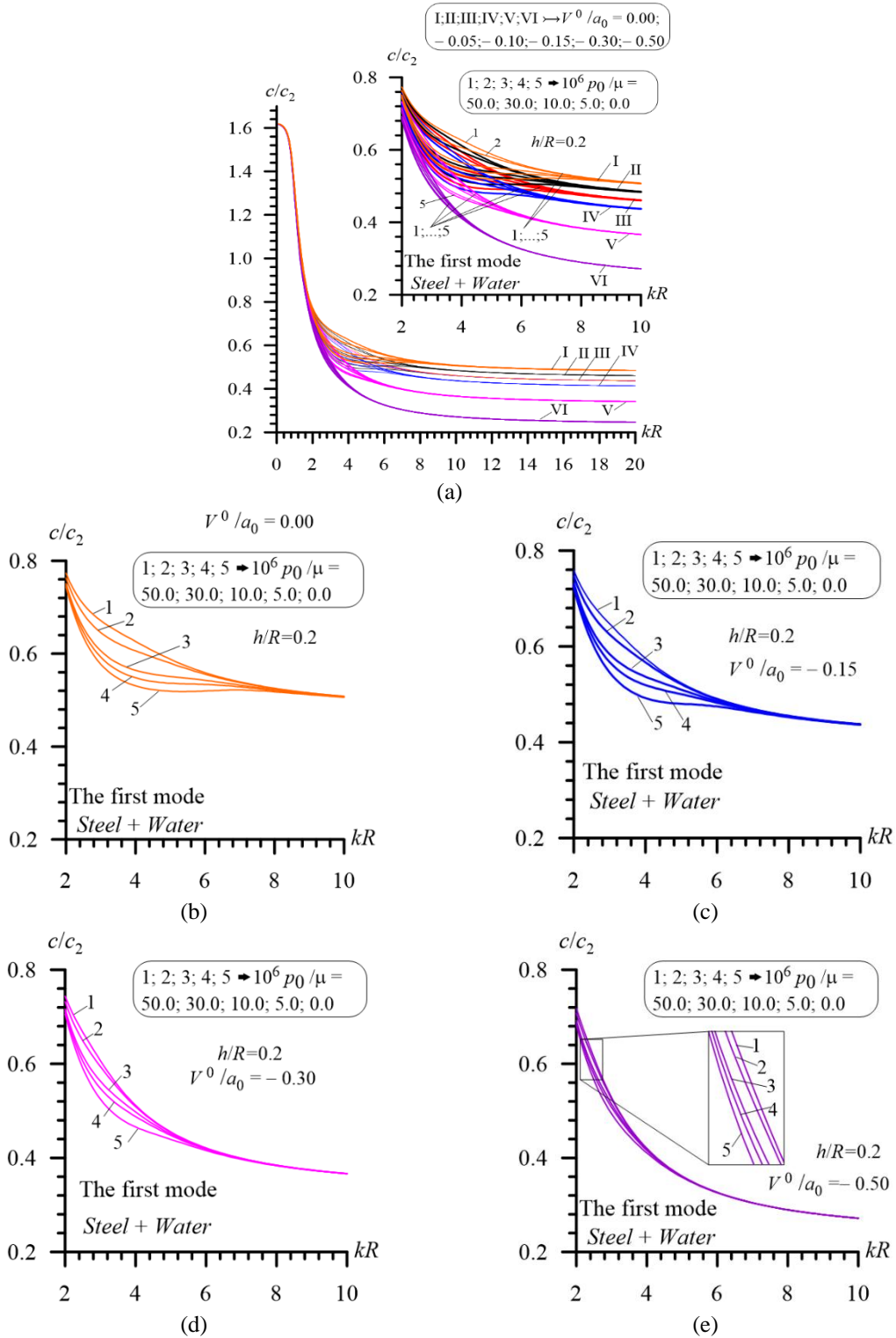
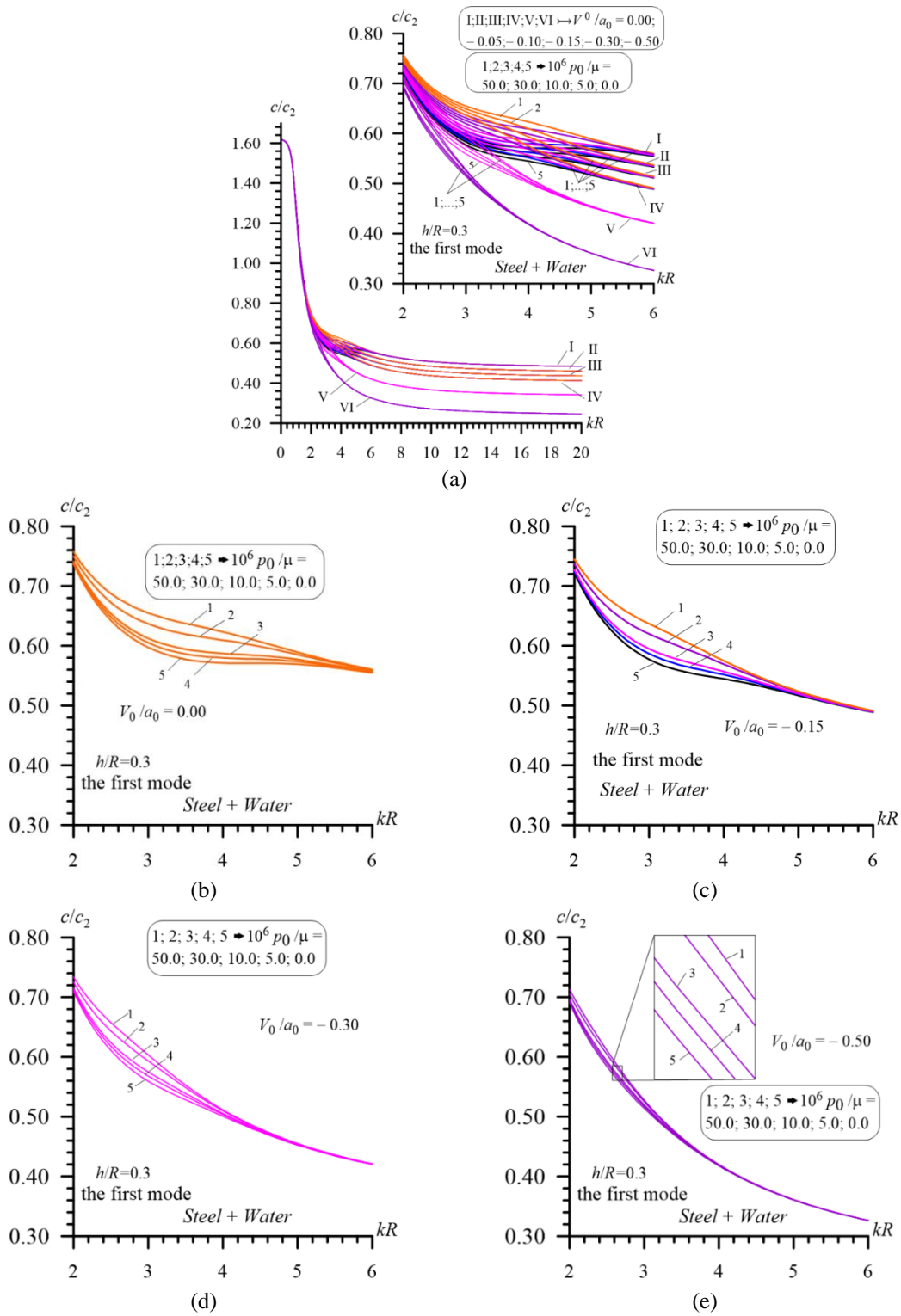Fig. 6 Dispersion curves for the first mode obtained under $h/R = 0.2$

Fig. 7 Dispersion curves for the first mode obtained under $h/R = 0.3$

h/R and the absolute values of the minus dimensionless velocity V^0/a_0. An increase in the values of the ratio h/R causes a decrease in the values of $(kR)'$. At the same time, in the first mode, an increase in the absolute values of the ratio V^0/a_0 leads not only to a decrease in the values of $(kR)'$, but also to a decrease in the magnitude of the influence of p_0/μ on the wave propagation velocity.

Now we attempt to explain the character of the dispersion curves related to the first mode. It follows from Figs. 5, 6, and 7 that under the low wavenumber approach (the cases where $0 < kR \leq 2.0$), the influence of the fluid flow velocity on the wave propagation velocity disappears almost completely.

According to the results obtained in the papers (Akbarov *et al.* 2021) and (Sinha *et al.*1992), in the low wavenumber approach, the dispersion curves of the first and the second modes obtained for the "cylinder+fluid" hydro-elastic system are very near to the corresponding dispersion curves obtained for the empty hollow cylinder. However, after a certain value of kR the dispersion curves of the first mode obtained for the "cylinder+fluid" hydro-elastic system separate from the corresponding dispersion curves related to the empty cylinder, and approach the first mode of the dispersion curves related to the waves propagating in the fluid cylinder, examples of which are constructed in Fig. 3. This explains the character of the influence of the fluid flow velocity and of the inhomogeneous initial stresses on the dispersion curves in the first mode.

Accordingly, the influence of the fluid flow velocity on the dispersion curves of the first mode begins after the aforementioned "certain value" of kR and, as a result of this flow, the wave propagation velocity decreases and the relations in (29) occur also for the first mode. At the same time, in the cases where $kR \geq 2.0$, the relations in (30) occur also for the first mode.

Note that all the results presented in Figs. 4-7 and obtained in the case where $V^0/a_0 = 0$ and $p_0/\mu \geq 0$ in particular cases coincide with the corresponding ones obtained in the paper (Akbarov *et al.* 2021). Moreover, in particular cases, the dispersion curves illustrated in these figures and constructed in the case where $p_0/\mu = 0$ and $V^0/a_0 \neq 0$ coincide with the corresponding dispersion curves constructed in the paper (Veliyev 2023). Note also that the paper (Veliyev 2023) considered only a few numerical results on the influence of the fluid flow on the dispersion curves of the axisymmetric waves propagating in the cylinder containing this fluid. What is more, these results are obtained when the cylinder has no initial stresses, and it is not an attempt to explain the character of this influence.

We recall that the numerical results discussed above are obtained in the case where $N = 54$. Now, we consider the convergence of the numerical results with this number of sub-intervals. For this purpose, we consider the numerical results in Fig. 8 which illustrate the dispersion curves of the first mode obtained for various numbers of sub-intervals N under $h/R = 0.3$, $V^0/a_0 = -0.15$ and $10^6 p_0/\mu = 50$. It follows from Fig. 8 that the selected number of sub-intervals even in the most unfavorable case provides convergence of the numerical results with high accuracy.

4.3 Numerical results obtained in the case where $V^0/a_0 > 0$

Now, we analyze the dispersion curves constructed in the case where the fluid flow direction in the initial state coincides with the wave propagation direction. We begin this analysis with the dispersion curves presented in Fig. 9 and related to the zeroth mode. Note that these curves are constructed in the cases where $h/R =0.05$ (Fig. 9(a)), 0.10 (Fig. 9(b)), and 0.20 (Fig. 9(c)), and we recall that the waves, to which these dispersion curves relate, are also named as "quasi-Scholte" waves.
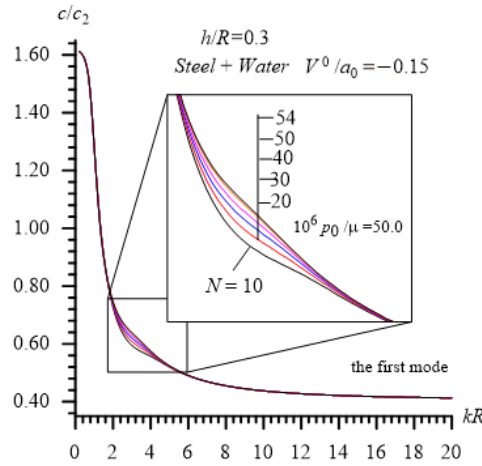
Fig. 8 Convergence of the numerical results with respect to the number N in the first mode under $h/R = 0.3$ and $V^0/a_0 = -0.15$

Thus, it follows from Fig. 9 that in the case where $V^0/a_0 > 0$, the fluid flow in the initial state leads to an increase in the wave propagation velocity, and the magnitude of this increase grows monotonically with V^0/a_0. Moreover, it follows from the results that the high wavenumber limit value of the quasi-Scholte waves (i.e., the velocity of the corresponding Scholte wave) depends significantly on the fluid flow velocity in the initial state. In light of the influence of the fluid flow velocity on the wave propagation velocity, we consider the dependence between this wave propagation velocity and initial inhomogeneous stresses, the magnitudes of which are estimated through the ratio p_0/μ.

Thus, it follows from Fig. 9 that, as in the case where $V^0/a_0 < 0$, an increase in the values of the ratio p_0/μ causes an increase in the values of the wave propagation velocity. However, in the present case, i.e., in the case where $V^0/a_0 > 0$, the magnitude of this influence increases significantly with V^0/a_0. This is the main qualitative difference of the action of the fluid flow velocity in the case where $V^0/a_0 > 0$ on the influence of the initial inhomogeneous stresses on the wave propagation velocity. We recall that, as shown in the previous subsection, in the case where $V^0/a_0 < 0$, this effect was the opposite.

Analysis of the numerical results illustrated in Fig. 9 allows us to write that for each selected value of the ratio p_0/μ the following relations take place

$$c/c_2|_{V^0/a_0=0.00} < c/c_2|_{V^0/a_0=0.05} < c/c_2|_{V^0/a_0=0.15} < c/c_2|_{V^0/a_0=0.30} < c/c_2|_{V^0/a_0=0.50} \quad (32)$$

Also, in the case where $V^0/a_0 > 0$ (as in the case where $V^0/a_0 < 0$), there exists such a value of kR (denote it by $(kR)*$) after which, i.e., in the cases where $kR > (kR)*$ (in the cases where $kR < (kR)*$) for each fixed value of the ratio V^0/a_0, as in (30), the following relations take place

$$c/c_2|_{10^6 p_0/\mu=0.0} < c/c_2|_{10^6 p_0/\mu=3.0} < c/c_2|_{10^6 p_0/\mu=10.0} < c/c_2|_{10^6 p_0/\mu=15.0}. \quad (33)$$

However, in the cases where $kR < (kR)*$, as in (31), the relations (33) become the opposite, i.e.

$$c/c_2|_{10^6 p_0/\mu=0.0} > c/c_2|_{10^6 p_0/\mu=3.0} > c/c_2|_{10^6 p_0/\mu=10.0} > c/c_2|_{10^6 p_0/\mu=15.0}. \quad (34)$$
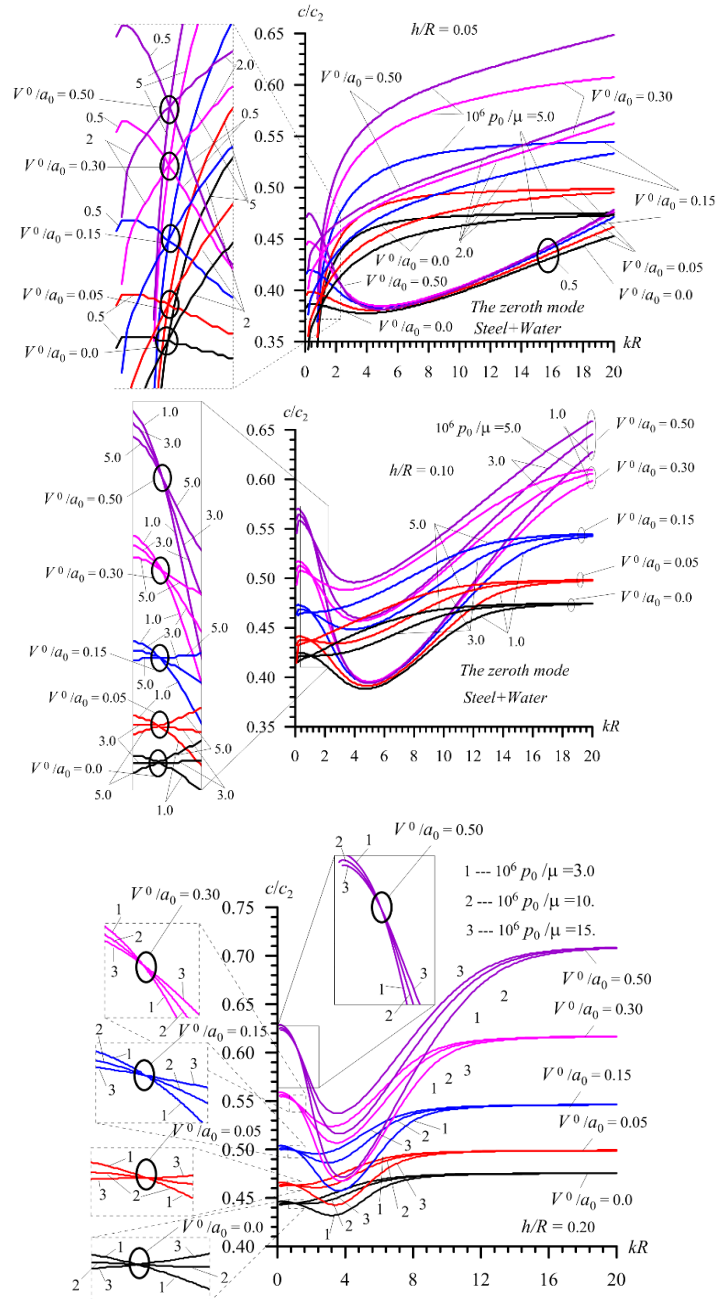
Fig. 9 Dispersion curves in the zeroth mode constructed for the case where $V^0/a_0 > 0$ under $h/R = 0.05$ (a), 0.1 (b) and 0.2 (c)

Note that the relations in (32) are opposite the corresponding relations in (29) which relate to the case where $V_0/a_0 < 0$. However, the relations in (33) and (34) agree in the qualitative sense with the relations in (30) and (31), respectively.
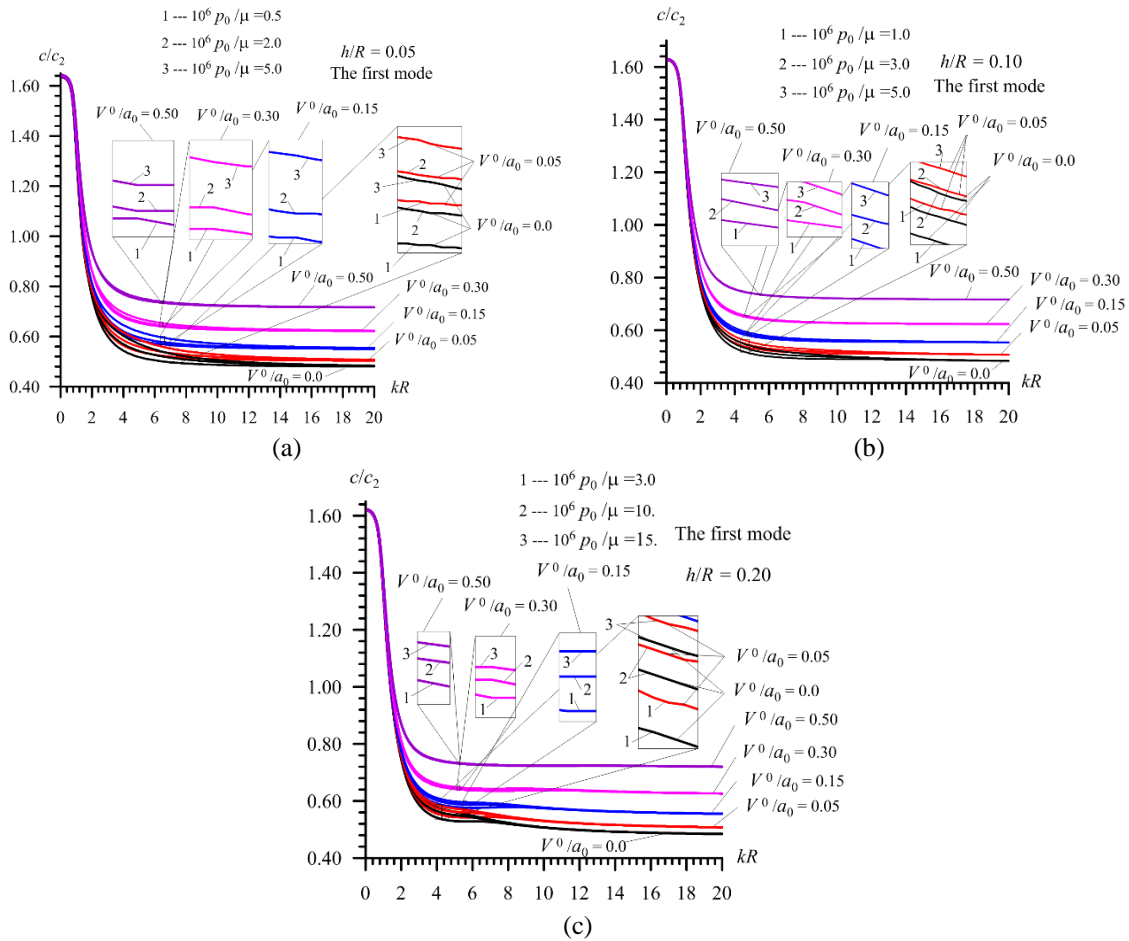
Fig. 10 Dispersion curves in the first mode constructed for the case where $V^0/a_0 > 0$ under $h/R = 0.05$ (a), 0.1 (b) and 0.2 (c)

Now, we analyze the dispersion curves related to the first mode. These curves are presented in Figs. 10 and 11. In Fig. 10, the graphs grouped by letters *a*, *b*, and *c* relate to the cases where $h/R =$ 0.05, 0.10, and 0.20, respectively. However, in Fig. 11, the graphs grouped by letters *a*, *b*, and *c* show the parts of the dispersion curves illustrated in Fig. 10 (a), (b), and (c), respectively in which the magnitude of the influence of the initial inhomogeneous stresses, i.e., of the ratio p_0/μ on the wave propagation velocity is considerable.

It follows from the results given in Figs. 10 and 11 that in the case where $V^0/a_0 > 0$, an increase in the values of the fluid flow velocity, as in the zeroth mode, leads to a monotonic increase in the wave propagation velocity. For each fixed value of V^0/a_0, an increase in the values of p_0/μ also causes an increase in the values of the wave propagation velocity. However, as in the case where $V^0/a_0 < 0$, a significant influence of the ratio p_0/μ on the wave propagation velocity is observed with certain values of the dimensionless wavenumber. Moreover, it follows from the results that in the case where $V^0/a_0 > 0$, the effect of an increase in the values of the ratio V^0/a_0 on a decrease of the magnitude of the influence of the ratio p_0/μ on the wave propagation velocity
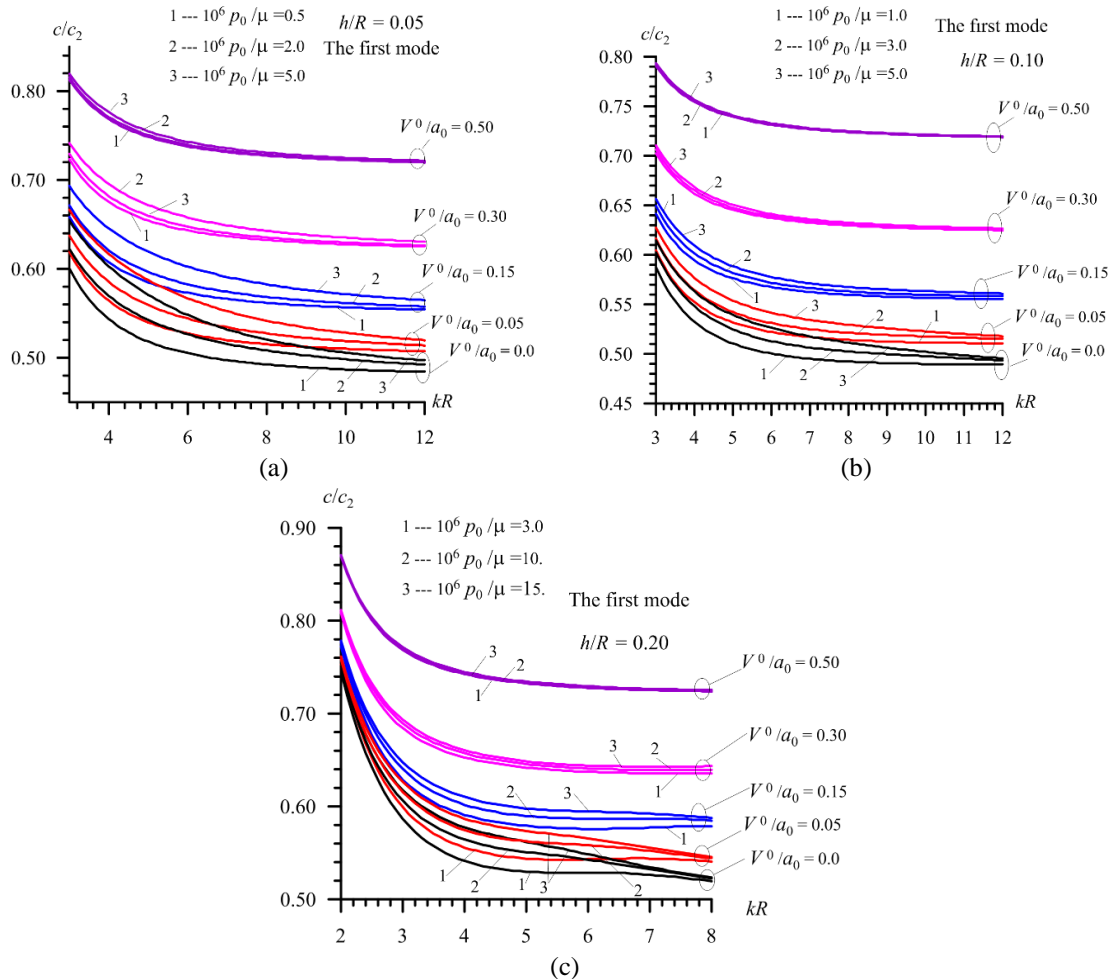
Fig. 11 The parts of the dispersion curves given in Figs. 10a (a), 10b (b), and 10c (c) in which the magnitude of the influence of the ratio p_0/μ on the dispersion curves is considerable

is more considerable than in the case where $V^0/a_0 < 0$. Note that the results obtained for the first mode in the case where $V^0/a_0 > 0$ in the qualitative sense agree with the corresponding results obtained in the paper (Deng and Yang 2013).

We again turn to the existence of the specific regions for the dimensionless wavenumber kR in which the influence of the effect of V^0/a_0 (> 0) on the magnitude of the influence of the ratio p_0/μ on the wave propagation velocity is more significant. The appearance of such regions can be explained by the dominant role of the elastic cylinder on the dispersion curves in the low wavenumber values and by the dominant role of the fluid on the dispersion curves in the high wavenumber values. As follows from Fig. 10, in the low wavenumber values of kR, the wave propagation velocity in the first mode approaches the wave propagation velocity in the corresponding empty cylinder with the inhomogeneous initial stresses. Moreover, the low wavenumber limit values of the velocity of the waves hardly depend on the fluid flow velocity in the initial state, i.e., on the ratio V^0/a_0.

However, in the high wavenumber values of kR, the wave propagation velocity approaches the corresponding wave propagation velocity in the fluid, which is in the rigid cylinder and flows in the initial state with the velocity V^0/a_0. We recall that the dispersion curves of these waves are illustrated in Fig. 3(b). Thus, it follows from Fig. 10 that the high wavenumber limit values of the wave propagation velocity hardly depend on the inhomogeneous initial stresses in the cylinder, i.e., on the ratio p_0/μ.

Thus, according to the above situations, a region appears between the low and high wavenumbers, in which the effect of the ratio V^0/a_0 on the magnitude of the influence p_0/μ on the wave propagation velocity becomes considerable. What is more, this region's size depends on the problem's parameters, the mode number, and the direction of the fluid flow velocity in the initial state.

The preceding explanations relate to the results obtained for the first mode where $V^0/a_0 > 0$ and $V^0/a_0 < 0$. However, some similar attempts to explain the results obtained in the case where $V^0/a_0 < 0$ and $p_0/\mu = 0$ were also made in subsection 4.1. We note that the preceding explanations cannot be applied to the results of the zeroth mode. The zeroth or quasi-Scholte mode results appear due to the fluid-elastic cylinder dynamic interaction. Nevertheless, in the high minus values of the ratio V^0/a_0, the influence of the contact of the fluid with the elastic cylinder on the wave propagation velocity almost disappears, and the dispersive zeroth mode becomes non-dispersive. Recall that this situation was also detailed in the previous subsection.

5. Conclusions

Thus, in the present paper, the influence of the fluid flow velocity and flow direction on the dispersion of the axisymmetric waves propagating in the inhomogeneous pre-stressed hollow cylinder containing this fluid is investigated. It is assumed that the material of the cylinder is linearly elastic and the fluid is a barotropic compressible inviscid one. Formulation of the corresponding eigenvalue problem is made within the scope of the so-called three-dimensional linearized theory of elastic waves in bodies with initial stresses and of the linearized Euler equations for a compressible inviscid fluid. For the solution to the corresponding field equations related to the cylinder, the discrete-analytical method is employed, according to which, the interval with respect to the radial coordinate is divided into a certain number of sub-intervals and within each sub-interval, the analytic solutions to these equations are found. The corresponding dispersion equation is derived from the boundary, compatibility and contact conditions between the sub-intervals. The dispersion equation is solved numerically, as a result of which the dispersion curves are constructed for various values of the problem parameters, which are mainly the initial inhomogeneous stresses in the cylinder and the initial flowing velocity of the fluid contained in this cylinder. These results are presented for the zeroth and first modes, and are obtained for the case in which the fluid flow direction is opposite to the direction of wave propagation, and in the case where the fluid flow direction coincides with the wave propagation direction. By analyzing these results, conclusions are drawn regarding the influence of the fluid flow velocity in the initial state on the wave propagation velocity in the considered hydro-elastic system. The attempt is also made to explain the character of the influence of the fluid flow velocity on the dispersion curves.

According to the obtained and analyzed numerical results, concrete conclusions on the character of the fluid flow velocity and fluid flow direction on the magnitude of the influence of the inhomogeneous initial stresses in the cylinder on the studied wave propagation velocity are

made. For instance, one such conclusion is the following: in the case where the fluid flow direction coincides with (is opposite) the wave propagation direction, an increase in the absolute values of the fluid flow velocity leads to an increase (a decrease) in the magnitude of the influence of the initial inhomogeneous stresses on the propagation velocity of the quasi-Scholte waves in the hydro-elastic system under consideration.

References

Akbarov, S.D. (2015), *Dynamics of Pre-strained Bi-material Elastic Systems: Linearized Three-Dimensional Approach*, Springer, Heidelberg, New York, USA.

Akbarov, S.D. (2018), "Forced vibration of the hydro-viscoelastic and-elastic systems consisting of the viscoelastic or elastic plate, compressible viscous fluid and rigid wall: A review", *Appl. Comput. Math.*, **17**(3), 221-245.

Akbarov, S.D. and Bagirov, E.T. (2019a), "Dispersion of axisymmetric longitudinal waves in a "hollow cylinder+surrounding medium" system with inhomogeneous initial stresses", *Struct. Eng. Mech.*, **72**(5), 597-615. http://doi.org/10.12989/sem.2019.72.5.597.

Akbarov, S.D. and Bagirov, E.T. (2019b), "Axisymmetric longitudinal wave dispersion in a bi-layered circular cylinder with inhomogeneous initial stresses", *J. Sound Vib.*, **450**, 1-27. https://doi.org/10.1016/j.jsv.2019.03.003.

Akbarov, S.D. and Bagirov, E.T. (2021), "The dispersion of the axisymmetric longitudinal waves propagating in the bi-layered hollow cylinder with the initial inhomogeneous thermal stresses", *Wave. Random Complex Media*, **34**(2), 471-509. https:/doi.org/10.1080/17455030.2021.1912437.

Akbarov, S.D. and Bagirov, E.T. (2024), "Dispersion of axisymmetric longitudinal waves propagating in an inhomogeneous prestressed hollow cylinder immersed in an inviscid compressible fluid", *J. Sound Vib.*, **569**, 118097. https://doi.org/10.1016/j.jsv.2023.118097.

Akbarov, S.D. and Veliyev, Q.J. (2023), "Parametric study of the wave dispersion in the hydro-elastic system consisting of an inhomogeneously prestressed hollow cylinder containing compressible inviscid fluid", *Couple. Syst. Mech.*, **12**(1), 41-68. https://doi.org/10.12989/csm.2023.12.1.041.

Akbarov, S.D., Sevdimaliyev, Y.M. and Valiyev, G.J. (2021), "Mathematical modeling of the dynamics of a hydroelastic system.A hollow cylinder with inhomogeneous initial stresses and compressible fluid", *Math. Meth. Appl. Sci.*, **44**(9), 7858-7872. https://doi.org/10.1002/mma.7329.

Atabek, H.B. (1968), "Wave propagation through a viscous fluid contained in a tethered initially stressed, orthotropic elastic tube", *Biophys. J.*, **8**, 626-649.

Atabek, H.B. and Lew, H.S. (1966), "Wave propagation through a viscous incompressible fluid contained in an initially stressed elastic tube", *Biophys. J.*, **6**, 481-503.

Bagno, A.M. (2017), "Dispersion properties of Lamb waves in an elastic layer-ideal liquid half-space system", *Int. Appl. Mech.*, **53**(6), 609-616. http://doi.org/10.1007/s10778-018-0843-9.

Bagno, A.M. and Guz, A.N. (1982), "Wave propagation in a previously stressed, incompressible cylinder containing a viscous compressible liquid", *Mech. Compos. Mater.*, **2**, 349-355.

Bagno, A.M. and Guz, A.N. (1997), "Elastic waves in prestressed bodies interacting with fluid (Survey)", *Int. Appl. Mech.*, **33**(6), 435-465. https://doi.org/10.1007/BF02700652.

Bagno, A.M. and Guz, A.N. (2016), "Effect of prestresses on the dispersion of waves in a system consisting of a viscous liquid layer and a compressible elastic layer", *Int. Appl. Mech.*, **52**(8), 333-341. https://doi.org/10.1007/s10778-016-0756-4.

Bagno, A.M., Guz, A.N. and Efremov, V.I. (1994), "Effect of initial strains on the propagation of waves in an incompressible cylinder located in an ideal fluid", *Int. Appl. Mech.*, **30**(8), 583-585. https://doi.org/10.1007/BF00847229.

Bagno, O.M. (2023), "Effect of prestresses on generalized lamb waves in an elastic compressible layer interacting with a viscous liquid layer", *Int. Appl. Mech.*, **59**(4), 417-428. https://doi.org/10.1007/s10778-

023-01232-y.

D.AKBAROV, S., Valiyev, G., Aliyev, S.A. and Khankishiyev, Z. (2024), "The influence of the inhomogeneous initial stresses in the hollow cylinder containing an inviscid fluid on the dispersion of the quasi-Scholte waves propagating in this cylinder", *Appl. Comput. Math.*, **23**(1), 18-39.

Deng, Q.T. and Yang, Z.Ch. (2013), "Wave propagation analysis in buried pipe conveying fluid", *Appl. Math. Model.*, **37**, 6225-6233. http://doi.org/10.1016/j.apm.2013.01.014.

Eringen, A.C. and Suhubi, E.S. (1975), *Elastodynamics, Finite Motion, Vol. I; Linear Theory, Vol. II*, Academic Press, New York.

Guz, A.N. (2004), *Elastic Waves in Bodies with Initial (Residual) Stresses*, A.C.K. Kyiv. (in Russian)

Guz, A.N. (2009), *Dynamics of Compressible Viscous Fluid*, Cambridge Scientific Publishers, Cambridge.

Guz, A.N. and Bagno, A.M. (2018), "Effect of prestresses on the dispersion of lamb waves in a system consisting of a viscous liquid layer and a compressible elastic layer", *Int. Appl. Mech.*, **54**(3), 249-258. https://doi.org/10.1007/s10778-018-0902-2.

Guz, A.N. and Bagno, A.M. (2019), "Propagation of quasi-lamb waves in an elastic layer interacting with a viscous liquid half-space", *Int. Appl. Mech.*, **55**(5), 459-469. https://doi.org/10.1007/s10778-019-00968-w.

Hadzalic, E., Ibrahimbegovic, A. and Dolarevic, S. (2018), "Fluid-structure interaction system redicting both internal pore pressure and outside hydrodynamic pressure", *Couple. Syst. Mech.*, **7**(6), 649-668. https://doi.org/10.12989/csm.2018.7.6.649.

Kocal, T. and Akbarov, S.D. (2017), "On the attenuation of the axisymmetric longitudinal waves propagating in the bi-layered hollow cylinder made of viscoelastic materials", *Struct. Eng. Mech.*, **61**(1), 145-165. http://doi.org/10.12989/sem.2017.61.1.143.

Kocal, T. and Akbarov, S.D. (2019), "The influence of the rheological parameters on the dispersion of the flexural waves in a viscoelastic bi-layered hollow cylinder", *Struct. Eng. Mech.*, **71**(5), 577-601. http://doi.org/10.12989/sem.2019.71.5.577.

Kubenko, V.D., Yanchevs'kyi, I.V., Zhuk, Y.O. and Liskin, V.O. (2023), "Hydrodynamic characteristics of a plane wave interacting with a spherical body in a semi-infinite cylindrical cavity filled with a compressible fluid", *Int. Appl. Mech.*, **59**, 131-144. https://doi.org/10.1007/s10778-023-01207-z.

Lamb, H. (1898), "On the velocity of sound in a tube, as affected by the elasticity of the walls", *Manchester Memoirs*, **42**(9), 1-16.

Lin, T.C. and Morgan, G.W. (1956), "Wave propagation through fluid contained in a cylindrical, elastic shell", *J. Acoust. Soc. Am.*, **28**(15), 1165-1176.

Negin, M. and Akbarov, S.D. (2019), "On attenuation of the seismic Rayleigh waves propagating in an elastic crustal layer over viscoelastic mantle", *J. Earth Syst. Sci.*, **128**(7), 181. https://doi.org/10.1007/s12040-019-1202-x.

Plona, T.J., Sinha, B.K., Kostek, S. and Chong, S.K. (1992), "Axisymmetric wave propagation in fluid loaded cylindrical shells. II. Theory versus experiment", *J. Acoust. Soc. Am.*, **92**(2), 1144-1155. https://doi.org/10.1121/1.404041.

Rvachev, A.I. (1978), "Propagation of a pulse wave in arteries taking account of prior stresses and muscle activity", *Mekh. Polim.*, **2**, 244-252.

Sandhyarani, B., Rao, J.A. and Reddy, P.M. (2019), "Axially symmetric vibrations of a liquid-filled poroelastic thin cylinder saturated with two immiscible liquids surrounded by a liquid", *J. Solid Mech.*, **11**(2), 272-280. https://doi.org/10.22034/JSM.2019.665907.

Selvamani, R. (2016), "Dispersion analysis in a fluid-filled and immersed transversely isotropic thermos-electro-elastic hollow cylinder", *Mech. Mech. Eng.*, **20**(3), 2009-2031.

Shah, S.A. (2008), "Axially symmetric vibrations of fluid-filled poroelastic circular cylindrical shells", *J. Sound Vib.*, **318**(1-2), 389-405. https://doi.org/10.1016/j.jsv.2008.04.012.

Sinha, B.K., Plona, T.J., Kostek, S. and Chong, S.K. (1992), "Axisymmetric wave propagation in fluid loaded cylindrical shells. I: Theory", *J. Acoust. Soc. Am.*, **92**(2), 1132-1143. https://doi.org/10.1121/1.404040.

Timoshenko, S. and Goodier, J.N. (1951), *Theory of Elasticity*, McGraw-Hill, New York.

Veliyev, G.J. (2023), "The influence of the fluid flow speed on the axisymmetric wave propagation velocity

in the cylinder containing this fluid", *IOSR J. Mech. Civil Eng. (IOSR-JMCE)*, **19**(6), 52-61. https://doi.org/10.9790/1684-1906015261.

Veliyev, Q.J. and Ipek, C. (2023), "The influence of the material properties of an inhomogeneous pre-stressed hollow cylinder containing an inviscid fluid on the dispersion of Quasi-Scholte waves", *Int. Appl. Mech.*, **59**, 619-629. https://doi.org/10.1007/s10778-024-01246-0.

Watson, G.N. (1966), *A Treatise on the Theory of Bessel Function*s, 2nd Edition, Cambridge University Press, Cambridge.

CC

Appendix A

In the present Appendix, the explicit expressions for displacements and stresses of the cylinder which enter the conditions in (14) are given through the formulae (A1) and (A2) in which the notation in (19)-(22) is used.

$$u_r^n(r) = A_1^n \frac{dr_2^n}{dr} \left[\gamma_1(r_n)(r_2^n)^{(\gamma_1(r_n)-1)} E_{\gamma_1(r_n)}(r_2^n) + (r_2^{(n)})^{\gamma_1(r_n)} \frac{dE_{\gamma_1(r_n)}(r_2^n)}{dr_2^n} \right] +$$

$$A_2^n \frac{dr_2^n}{dr} \left[\gamma_1(r_n)(r_2^n)^{(\gamma_1(r_n)-1)} F_{\gamma_1(r_n)}(r_2^n) + (r_2^n)^{\gamma_1(r_n)} \frac{dF_{\gamma_1(r_n)}(r_2^n)}{dr_2^n} \right] +$$

$$B_1^n \frac{dr_1^n}{dr} \left[\gamma(r_n)(r_1^n)^{(\gamma(r_n)-1)} E_{\gamma(r_n)}(r_1^n) + \right.$$

$$\left. (r_1^n)^{\gamma(r_n)} \frac{dF_{\gamma(r_n)}(r_1^n)}{d(r_1^n)} \right] + B_2^n \frac{dr_1^n}{dr} \left[\gamma(r_n)(r_1^n)^{(\gamma(r_n)-1)} F_{\gamma(r_n)}(r_1^n) + (r_1^n)^{\gamma(r_n)} \frac{dF_{\gamma(r_n)}(r_1^n)}{d(r_1^n)} \right],$$

$$u_z^n(r) = A_1^n (r_2^n)^{\gamma_1(r_n)} E_{\gamma_1(r_n)}(r_2^n) + A_2^n (r_2^n)^{\gamma_1(r_n)} F_{\gamma_1(r_n)}(r_2^n) - \qquad \text{(A1)}$$

$$B_1^n \left[\gamma(r_n)(\gamma(r_n)-1) \left(\frac{dr_2^n}{dr} \right)^2 E_{\gamma(r_n)}(r_1^n) + \gamma(r_{n_i})(r_1^n)^{(\gamma(r_n)-1)} \times \frac{1}{r} E_{\gamma(r_n)}(r_1^n) + \right.$$

$$\left. 2\gamma(r_n) \left(\frac{dr_1^n}{dr} \right)^2 \times \frac{dE_{\gamma(r_n)}(r_1^n)}{d(r_1^n)} + \frac{1}{r}(r_1^n)^{\gamma(r_n)} \times \frac{dr_1^n}{dr} \frac{dE_{\gamma(r_n)}(r_1^n)}{d(r_1^n)} + (r_1^n)^{\gamma(r_n)} \left(\frac{dr_1^n}{dr} \right)^2 \frac{d^2 E_{\gamma(r_n)}(r_1^n)}{d(r_1^n)^2} \right] -$$

$$B_2^n \left[\gamma(r_n)(\gamma(r_n)-1) \left(\frac{dr_2^n}{dr} \right)^2 F_{\gamma(r_n)}(r_1^n) + \gamma(r_n)(r_1^n)^{(\gamma(r_n)-1)} \times \frac{1}{r} F_{\gamma(r_n)}(r_1^n) + \right.$$

$$\left. 2\gamma(r_n) \left(\frac{dr_1^n}{dr} \right)^2 \times \frac{dF_{\gamma(r_n)}(r_1^n)}{d(r_1^n)} + \frac{1}{r}(r_1^n)^{\gamma(r_n)} \frac{dr_1^n}{dr} \frac{dF_{\gamma(r_n)}(r_1^n)}{d(r_1^n)} + (r_1^n)^{\gamma(r_n)} \left(\frac{dr_1^n}{dr} \right)^2 \frac{d^2 F_{\gamma(r_n)}(r_1^n)}{d(r_1^n)^2} \right]$$

$$\frac{\sigma_{rr}^n(r)}{\mu} = A_1^n \left\{ \left(\frac{dr_2^n}{dr} \right)^2 2\left(1 + \frac{\lambda}{2\mu} \right) \times \left[\gamma_1(r_n)(\gamma_1(r_n)-1)(r_2^n)^{(\gamma_1(r_n)-2)} E_{\gamma_1(r_n)}(r_2^n) + \right. \right.$$

$$2\gamma_1(r_n)(r_2^n)^{(\gamma_1(r_n)-1)} \frac{dE_{\gamma_1(r_n)}(r_2^n)}{d(r_2^n)} +$$

$$(r_2^n)^{\gamma_1(r_n)} \frac{d^2 E_{\gamma_1(r_n)}(r_2^n)}{d(r_2^n)^2} \right] + \frac{\lambda}{\mu} \frac{1}{r_2^n} \left(\frac{dr_2^n}{dr} \right)^2 \left[\gamma_1(r_n)(r_2^n)^{(\gamma_1(r_n)-1)} E_{\gamma_1(r_n)}(r_2^n) + r_2^n \frac{dE_{\gamma_1(r_n)}(r_2^n)}{d(r_2^n)} \right] +$$

$$\frac{\lambda}{\mu} (r_2^n)^{\gamma_1(r_n)} E_{\gamma_1(r_n)}(r_2^n) \right\} + A_2^n \left\{ \left(\frac{dr_2^n}{dr} \right)^2 2\left(1 + \frac{\lambda}{2\mu} \right) \times \right.$$

$$\left[\gamma_1(r_n)(\gamma_1(r_n)-1)(r_2^n)^{(\gamma_1(r_n)-2)} F_{\gamma_1(r_n)}(r_2^n) + 2\gamma_1(r_n)(r_2^n)^{(\gamma_1(r_n)-1)} \frac{dF_{\gamma_1(r_n)}(r_2^n)}{d(r_2^n)} + \right.$$

$$(r_2^n)^{\gamma_1(r_n)} \frac{d^2 F_{\gamma_1(r_n)}(r_2^n)}{d(r_2^n)^2} + \frac{\lambda}{\mu} \frac{1}{r_2^n} \left(\frac{dr_2^{n_i}}{dr} \right)^2 \left[\gamma_1(r_n)(r_2^n)^{(\gamma_1(r_n)-1)} F_{\gamma_1(r_n)}(r_2^n) + r_2^n \frac{dF_{\gamma_1(r_n)}(r_2^n)}{d(r_2^n)} \right] +$$

$$\frac{\lambda}{\mu} (r_2^n)^{\gamma_1(r_n)} F_{\gamma_1(r_n)}(r_2^n) \right\} + B_1^n \left\{ \left(\frac{dr_1^n}{dr} \right)^2 2\left(1 + \frac{\lambda}{2\mu} \right) [\gamma(r_n)(\gamma(r_n)-1) \times \right.$$

$$(r_1^n)^{(\gamma(r_n)-2)} E_{\gamma(r_n)}(r_1^n) + 2\gamma(r_n)(r_1^n)^{(\gamma(r_n)-1)} \times \frac{dE_{\gamma_1(r_n)}(r_1^n)}{d(r_1^n)} + (r_1^n)^{\gamma(r_n)} \frac{d^2 E_{\gamma(r_n)}(r_1^n)}{d(r_1^n)^2} \right] +$$

$$\frac{\lambda}{\mu} \frac{1}{r_1^n} \left(\frac{dr_1^n}{dr} \right)^2 \left[\gamma(r_n)(r_1^n)^{(\gamma(r_n)-1)} E_{\gamma(r_n)}(r_1^n) + r_1^n \frac{dE_{\gamma(r_n)}(r_1^n)}{d(r_1^n)} \right] + \frac{\lambda}{\mu} [\gamma(r_n)(\gamma(r_n) -$$

$$1)(r_1^n)^{(\gamma(r_n)-2)} E_{\gamma(r_n)}(r_1^n) + \gamma(r_n)(r_1^n)^{(\gamma(r_n)-1)} \frac{1}{r_1^n} \left(\frac{dr_1^n}{dr} \right)^2 E_{\gamma(r_n)}(r_1^n) +$$

$$2\gamma(r_n)(r_1^n)^{(\gamma(r_n)-1)} \times \left(\frac{dr_1^n}{dr} \right)^2 \frac{dE_{\gamma(r_n)}(r_1^n)}{d(r_1^n)} + \frac{1}{r_1^n} \left(\frac{dr_1^n}{dr} \right)^2 \times (r_1^n)^{\gamma(r_n)} \frac{dE_{\gamma(r_n)}(r_1^n)}{d(r_1^n)} +$$

$$\left(\frac{dr_1^n}{dr} \right)^2 (r_1^n)^{\gamma(r_n)} \frac{d^2 E_{\gamma(r_n)}(r_1^n)}{d(r_1^n)^2} \right\} + B_2^n \left\{ \left(\frac{dr_1^n}{dr} \right)^2 2\left(1 + \frac{\lambda}{2\mu} \right) [\gamma(r_n)(\gamma(r_n)-1) \times \right.$$

$$(r_1^n)^{(\gamma(r_n)-2)} F_{\gamma(r_n)}(r_1^n) + 2\gamma(r_n)(r_1^n)^{(\gamma(r_n)-1)} \frac{dF_{\gamma(r_n)}(r_1^n)}{d(r_1^n)} + (r_1^n)^{\gamma(r_n)} \frac{d^2 F_{\gamma(r_n)}(r_1^n)}{d(r_1^n)^2}\Big] +$$

$$\frac{\lambda}{\mu}\frac{1}{r_1^n}\left(\frac{dr_1^n}{dr}\right)^2 \left[\gamma(r_n)(r_1^n)^{(\gamma(r_n)-1)} F_{\gamma(r_n)}(r_1^n) + r_1^n \frac{dF_{\gamma(r_n)}(r_1^n)}{d(r_1^n)}\right] + \frac{\lambda}{\mu}\left[\gamma(r_n)(\gamma(r_n) - \right.$$

$$1)(r_1^n)^{(\gamma(r_n)-2)} F_{\gamma(r_n)}(r_1^n) + \gamma(r_n)(r_1^n)^{(\gamma(r_n)-1)} \frac{1}{r_1^n}\left(\frac{dr_1^n}{dr}\right)^2 F_{\gamma(r_n)}(r_1^n) +$$

$$2\gamma(r_n)(r_1^n)^{(\gamma(r_n)-1)}\left(\frac{dr_1^n}{dr}\right)^2 \frac{dF_{\gamma(r_n)}(r_1^n)}{d(r_1^n)} + \frac{1}{r_1^n}\left(\frac{dr_1^n}{dr}\right)^2 (r_1^n)^{\gamma(r_n)} \frac{dF_{\gamma(r_n)}(r_1^n)}{d(r_1^n)} +$$

$$\left(\frac{dr_1^n}{dr}\right)^2 (r_1^n)^{\gamma(r_n)} \frac{d^2 F_{\gamma(r_n)}(r_1^n)}{d(r_1^n)^2}\Big]\Big\},$$

$$\frac{\sigma_{rz}^m(r)}{\mu} = A_1^n 2\frac{dr_2^n}{dr}\left[\gamma_1(r_n)(r_2^n)^{(\gamma_1(r_n)-1)} \times E_{\gamma 1(r_n)}(r_2^n) + (r_2^n)^{\gamma 1(r_n)} \frac{dE_{\gamma 1(r_n)}(r_2^n)}{d(r_2^n)}\right] +$$

$$A_2^n 2\frac{dr_2^n}{dr}\left[\gamma_1(r_n)(r_2^n)^{(\gamma_1(r_n)-1)} F_{\gamma_1(r_n)}(r_2^n) + (r_2^n)^{\gamma 1(r_n)} \frac{dF_{\gamma 1(r_n)}(r_2^n)}{d(r_2^n)}\right] + B_1^n\{-[\gamma(r_n)(\gamma(r_n) - \right.$$

$$1)(\gamma(r_n) - 2)E_{\gamma(r_n)}(r_1^n) +$$

$$3\gamma(r_n)(\gamma(r_n) - 1)(r_1^n)^{(\gamma(r_n)-2)}\left(\frac{dr_1^n}{dr}\right)^3 \times \frac{dE_{\gamma(r_n)}(r_1^n)}{d(r_1^n)} + 3\gamma(r_n)(r_1^n)^{(\gamma(r_n)-1)}\left(\frac{dr_1^n}{dr}\right)^3 \times$$

$$\frac{d^2 E_{\gamma(r_n)}(r_1^n)}{d(r_1^n)^2} + (r_1^n)^{\gamma(r_n)}\left(\frac{dr_1^n}{dr}\right)^3 \times \frac{d^3 E_{\gamma(r_n)}(r_1^n)}{d(r_1^n)^3} - \frac{1}{(r_1^n)^2}\gamma(r_n)(r_1^n)^{(\gamma(r_n)-1)} \times$$

$$\left(\frac{dr_1^n}{dr}\right)^3 E_{\gamma(r_n)}(r_1^n) - \frac{1}{(r_1^n)^2}\gamma(r_n)(r_1^n)^{\gamma(r_n)}\left(\frac{dr_1^n}{dr}\right)^3 \times \frac{dE_{\gamma(r_n)}(r_1^n)}{d(r_1^n)} + \gamma(r_n)(\gamma(r_n) - 1) \times \qquad (A2)$$

$$\frac{1}{r_1^n}(r_1^n)^{(\gamma(r_n)-2)}\left(\frac{dr_1^n}{dr}\right)^3 E_{\gamma(r_n)}(r_1^n) + 2\gamma(r_n)\left(\frac{dr_1^n}{dr}\right)^3 \frac{1}{r_1^n}\frac{dE_{\gamma(r_n)}(r_1^n)}{d(r_1^n)} +$$

$$\frac{1}{r_1^n}(r_1^n)^{\gamma(r_n)}\left(\frac{dr_1^n}{dr}\right)^3 \frac{d^2 E_{\gamma(r_n)}(r_1^n)}{d(r_1^n)^2}\Big] \frac{dr_1^n}{dr}[\gamma(r_n)(r_1^n)^{(\gamma(r_n)-1)} E_{\gamma(r_{n_i})}(r_1^n) +$$

$$(r_1^n)^{(\gamma(r_n)-1)} \frac{dE_{\gamma(r_n)}(r_1^n)}{d(r_1^n)}\Big]\Big\} + B_2^n\{-[\gamma(r_n)(\gamma(r_n) - 1)(\gamma(r_n) - 2) \times$$

$$F_{\gamma(r_n)}(r_1^n) + 3\gamma(r_n)(\gamma(r_n) - 1)(r_1^n)^{(\gamma(r_n)-2)} \times \left(\frac{dr_1^n}{dr}\right)^3 \frac{dE_{\gamma(r_n)}(r_1^n)}{d(r_1^{n_i})} +$$

$$3\gamma(r_n)(r_1^n)^{(\gamma(r_n)-1)}\left(\frac{dr_1^n}{dr}\right)^3 \times \frac{d^2 F_{\gamma(r_n)}(r_1^n)}{d(r_1^n)^2} + (r_1^n)^{\gamma(r_n)}\left(\frac{dr_1^n}{dr}\right)^3 \frac{d^3 F_{\gamma(r_n)}(r_1^n)}{d(r_1^n)^3} -$$

$$\frac{1}{(r_1^n)^2}\gamma(r_n)(r_1^n)^{(\gamma(r_n)-1)}\left(\frac{dr_1^n}{dr}\right)^3 F_{\gamma(r_n)}(r_1^n) - \frac{1}{(r_1^n)^2}\gamma(r_n)(r_1^n)^{\gamma(r_n)}\left(\frac{dr_1^n}{dr}\right)^3 \frac{dF_{\gamma(r_n)}(r_1^n)}{d(r_1^n)} +$$

$$\gamma(r_n)(\gamma(r_n) - 1) \times \frac{1}{r_1^n}(r_1^n)^{(\gamma(r_n)-2)}\left(\frac{dr_1^n}{dr}\right)^3 F_{\gamma(r_n)}(r_1^n) + 2\gamma(r_n)\left(\frac{dr_1^n}{dr}\right)^3 \frac{1}{r_1^n}\frac{dF_{\gamma(r_n)}(r_1^n)}{d(r_1^{n_i})} +$$

$$\frac{1}{r_1^n}(r_1^n)^{\gamma(r_n)}\left(\frac{dr_1^n}{dr}\right)^3 \frac{d^2 F_{\gamma(r_n)}(r_1^n)}{d(r_1^n)^2}\Big] + \frac{dr_1^n}{dr}[\gamma(r_n)(r_1^n)^{(\gamma(r_n)-1)} F_{\gamma(r_n)}(r_1^n) +$$

$$(r_1^n)^{(\gamma(r_n)-1)} \frac{dF_{\gamma(r_n)}(r_1^n)}{d(r_1^{n_i})}\Big]\Big\}.$$

The functions $E_x(y)$ and $F_x(y)$ in (A1) and (A2) are determined through the expressions in (22).